FMUC FACULDADE DE MEDICINA
UNIVERSIDADE DE COIMBRA

INSTITUTO GULBENKIAN DE CIÊNCIA

# INFLUENZA A VIRUS MODULATION OF CYTOKINES RELEASE FROM MACROPHAGES

**Joana Filipa Almeida Perdigão**

Dissertação de Mestrado apresentada à Faculdade de Medicina da Universidade de Coimbra em Investigação Biomédica

**2017**

**Orientador | Maria João Amorim, PhD; Colin Adrain, PhD**

**Coorientador | Henrique Girão, PhD**

**Supervisor | Marta Alenquer, PhD**

## ACKNOWLEDGEMENTS

First of all, I would like to express my sincere gratitude to Dr. Maria João Amorim, who encouraged me to pursue this project, for her patience, motivation and immense knowledge. Thanks you for giving me the opportunity to work in one of the best places to do science in Portugal, the Instituto Gulbenkian de Ciência.

I would like to acknowledge the valuable input of Dr. Colin Adrain, who contributed to my evolution and help in the shape of this project. During this time, I had the chance to develop my critical thinking and learn a great number of laboratorial techniques.

Next, I want to thank to my supervisors Sílvia, Filipe and especially to Marta for her patience, kindness and availability. Besides all of important scientific knowledge that I gained with you, thank you for teaching me the meaning of work in a team with so much professionalism.

I would further like to acknowledge the remaining members of Cell Biology of Viral infection and Membrane traffic groups. Zoé, Miguel, Emma and Inês thank you for the support and availability. Marina thank you for all the help, patience and friendship. And Nuno, thanks you for being a true friend.

I would like to thank to Ana Regalado for her permanent empathy, encouragement and friendship.

Just as importantly, I would like to express my very profound gratitude to my parents for the unconditional support, encouragement, love, endless patience and inspiration throughout my life. Thank you for giving me a pillar in times of need despite the long distance between us.

Finally, I would further acknowledge my friends and my boyfriend Daniel for providing me with unfailing support and continuous encouragement throughout the process of researching and writing this thesis. This accomplishment would not have been possible without them.

## ABSTRACT

Tumour necrosis factor α (TNF-α) is a pleiotropic cytokine produced by several types of cells and it plays fundamental roles in the healthy and diseased organism. Macrophages are the primary producers of TNFα upon injury, and its secretion is essential to the induction of a pro-inflammatory state necessary to resolve the assault. In activated macrophages, upon sensing an assault, TNFα is transcribed *de novo*, translated in ribosomes attached the endoplasmatic reticulum (ER) and transported to the plasma membrane using specific arms of the secretory pathway to be secreted upon cleavage by the protease TACE. It was reported that TNF-α was transported to the cell surface using the recycling endosome pathway and requiring the small GTPase Rab11.

Influenza A virus (IAV) is one of the most important human pathogens responsible for acute respiratory disease provoking seasonal epidemics and periodic pandemics. As any other virus, IAV must use the host machinery for every stage of its viral life-cycle. It was shown that during infection, IAV hijacks the recycling endosome to transport progeny RNAs (vRNPs) to the surface, requiring the small GTPase Rab11. vRNP binding to Rab11-vesicles causes alterations to the pathway, impairing the flow of vesicles and originating vesicular clustering.

The goal of this work was to merge both concepts to understand infected macrophages were deficient in the secretion of TNFα. Part of the project required the characterization of infection in macrophages and the elucidation of whether Rab11 was required to transport vRNPs in this system. Subsequently our aim was to investigate if the viral usage of Rab11 was in addition to transporting vRNPs a strategy for immune evasion, by analysing if TNFα trafficking in macrophages was modulated by IAV infection.

Our results indicate that Raw macrophages are permissive to viral infection and that the vRNPs are transported by Rab11-positive vesicles to reach the cell surface in these cells. However, our data strongly suggest that TNFα trafficking in macrophages does not rely on Rab11. Our conclusions were based in the usage of several viral strains that modulate at different levels the TNFα expression by suppressing to distinct extents innate immune responses from the host.

## SUMÁRIO

O fator de necrose tumoral alfa (TNFα) é uma citoquina pleiotrópica produzida por diversos tipos celulares. Esta proteína tem um papel fundamental quer em indivíduos saudáveis quer em indivíduos doentes. Os macrófagos são os principais produtores de TNFα quando estes sofrem algum tipo de insulto. A secreção de TNFα por parte dos macrófagos é essencial na indução de uma resposta pro-inflamatória que irá travar o insulto sofrido. Em macrófagos ativados, o TNFα é transcrito *de novo,* traduzido em ribossomas ligados ao reticulo endoplasmático e transportado para a membrana plasmática usando vias de secreção específicas. Uma vez chegado à superfície celular, o TNFα sofre clivagem proteolítica por parte da proteína TACE. Para chegar à superfície celular, tem sido descrito que o TNFα usa a via da reciclagem ligando-se a uma proteína GTPase conhecida por Rab11.

O vírus influenza A (IAV) é um importante patogeno humano, responsável por causar doença respiratória aguda provocando epidemias sazonais e pontualmente algumas pandemias. Tal como qualquer outro vírus, o IAV usa em sua vantagem, toda a maquinaria do hospedeiro em cada passo do seu ciclo viral. Durante a infeção, o IAV usa a via da reciclagem para transportar os seus vRNPs até à superfície ligando-se a uma pequena GTPase, a Rab11. Esta ligação causa severas alterações nesta via de secreção, irrompendo com o normal funcionamento das vesículas o que leva à formação de agregados vesiculares.

O objetivo último deste trabalho foi combinar estes dois conceitos e compreender se macrófagos infetados têm uma secreção deficiente em TNFα. Parte deste projeto requereu a caracterização da infeção em macrófagos e a confirmação relativamente à importância da Rab11 no transporte de vRNPs neste novo sistema. Assim fomos investigar se o uso da Rab11 por parte do vírus no transporte de vRNPs representa uma estratégia para evadir o sistema imune do hospedeiro através da analise da secreção de TNFα em macrófagos infetados por IAV. Os nossos resultados indicam que os macrófagos Raw264.7 são permissivos à infeção viral e que os vRNPs são transportados até à superfície celular através de vesículas de Rab11 nestas células. No entanto, a nossa analise indica fortemente que o TNFα não depende da Rab11 para ser transportado até à membrana plasmática nos macrófagos usados. As nossas conclusões são baseadas no uso de diversas estirpes do vírus que modulam diferentes níveis da expressão de TNFα através da supressão da resposta imune inata do hospedeiro.

# CONTENTS

# LIST OF TABLES AND FIGURES

## ABBREVIATIONS

| | |
|---|---|
| **CA** | Constitutively active |
| **cDNA** | Complementary DNA |
| **DN** | Dominant negative |
| **DNA** | Deoxyribonucleic acid |
| **ELISA** | Enzyme-Linked Immunosorbent Assay |
| **ER** | Endoplasmic reticulum |
| **FACS** | Fluorescence-Activated cell sorting |
| **GAPDH** | Glyceraldehyde 3-phosphate dehydrogenase protein |
| **H or HA** | Hemagglutinin |
| **IAV** | Influenza A virus |
| **IFN** | Interferon |
| **LPS** | Lipopolysaccharide |
| **M1** | Matrix protein 1 |
| **M2** | Matrix protein 2 |
| **MDCK** | Madin-Darby canine kidney cells |
| **MFI** | Mean Fluorescence intensity |
| **MOI** | Multiplicity of infection |
| **mRNA** | Messenger RNA |
| **N or NA** | Neuraminidase |
| **NEP** | Nuclear export protein |
| **NP** | Nucleoprotein |
| **p.i.** | Post-infection |
| **PA** | Polymerase acidic protein |
| **PB1** | Polymerase basic subunit 1 |
| **PB2** | Polymerase basic subunit 2 |
| **PFU** | Plaque forming unit |
| **PRR** | Pattern recognition receptor |
| **RE** | Recycling endosome |
| **RIG-I** | Retinoic acid-inducible gene 1 |
| **RNA** | Ribonucleic acid |
| **RT- qPCR** | Quantitative real time polymerase chain reaction |
| **TACE** | TNF alpha converting enzyme |
| **TGN** | Trans-Golgi network |
| **TLR** | Toll-like receptor |
| **TNF-R1** | TNF receptor 1 |
| **TNF-R2** | TNF receptor 2 |
| **TNFα** | Tumour necrosis factor alpha |

| | |
|---|---|
| **vRNA** | Viral RNA |
| **vRNP** | Viral ribonucleoprotein |
| **WT** | Wild-type |

# 1. Introduction

## 1.1. Tumour necrosis factor alpha (TNFα)

Tumour necrosis factor alpha (TNFα) was discovered more than a century ago by a German physician, P. Bruns[1]. TNFα is a pleiotropic cytokine that belongs to a superfamily of TNF proteins consisting of 19 members that signal through 29 receptors[2]. TNF superfamily cytokines regulate functions including immune responses, morphogenesis and haematopoiesis. However, they have also been implicated in tumorigenesis, septic shock, transplant rejection, bone resorption, rheumatoid arthritis and diabetes[3]. This indicates that the TNFα superfamily, and TNF specifically, have both beneficial and harmful roles.

TNFα is synthesized by a variety of tissues, including lymphoid cells, mast cells, endothelial cells, fibroblasts and neuronal tissue[4]. However, activated macrophages are the primary producers of TNFα in response to several factors such as injury, bacteria, viruses, complement factors, ischemia or hypoxia, orchestrating the production of a proinflammatory cascade[5].

TNFα when released binds to various cell types. All known responses of released TNFα are triggered by binding one of two transmembrane receptors on specific cells: TNF receptor 1 (TNF-R1) and TNF receptor 2 (TNF-R2) which are differentially regulated on various cell types in normal and diseased tissue[6,5] Whereas, TNF-R1 is, mostly, presented in immune cells (macrophages, NK, T and B cells), TNF-R2 is presented in both, immune cells and endothelial cells[7]. Some reports indicate that TNF-R1 mediates apoptosis and TNF-R2 mediates proliferations. However, others suggest that the two TNF-Rs transduce their signals cooperatively[8].

TNFα has both beneficial and harmful effects. TNFα is known by its anticancer potential mainly because of its systemic toxicity[9]. It also has a role in regulating the immune system contributing, for instance, to the function of cytotoxic effector cells in the recognition and destruction of virus-infected cells[4]. TNFα is also important in haematopoiesis and in protection against microbial infection[10].

Apart of the beneficial effects, TNFα has a role in several diseases. TNFα can contribute to tumorigenesis, participating in proliferation, invasion and metastasis of the tumours[3]. In autoimmunity, TNFα has been implicated in type II diabetes and rheumatoid arthritis. Moreover, TNFα is associated with chronic heart failure, bone resorption, AIDS, Alzheimer's disease, atherosclerosis and hepatotoxicity[11]. Figure 1.1 combines the main physiological and pathological effects of TNF.

For the reasons mentioned above, it is clear that TNFα and its receptors play important roles in many physiological functions. These roles have been explored to develop new therapies. TNFα is used to treat sarcomas and melanomas. In Crohn's disease, antibodies specific for TNFα have been used

and anti-TNFα therapy using TNF-R2 was approved to rheumatoid arthritis[12,13]. In fact, anti-TNF drugs are the highest selling biologics globally.

Although TNFα is a key factor in several biological processes, the molecular mechanisms promoting the cellular trafficking of TNFα and its subsequent secretion remain poorly characterised.

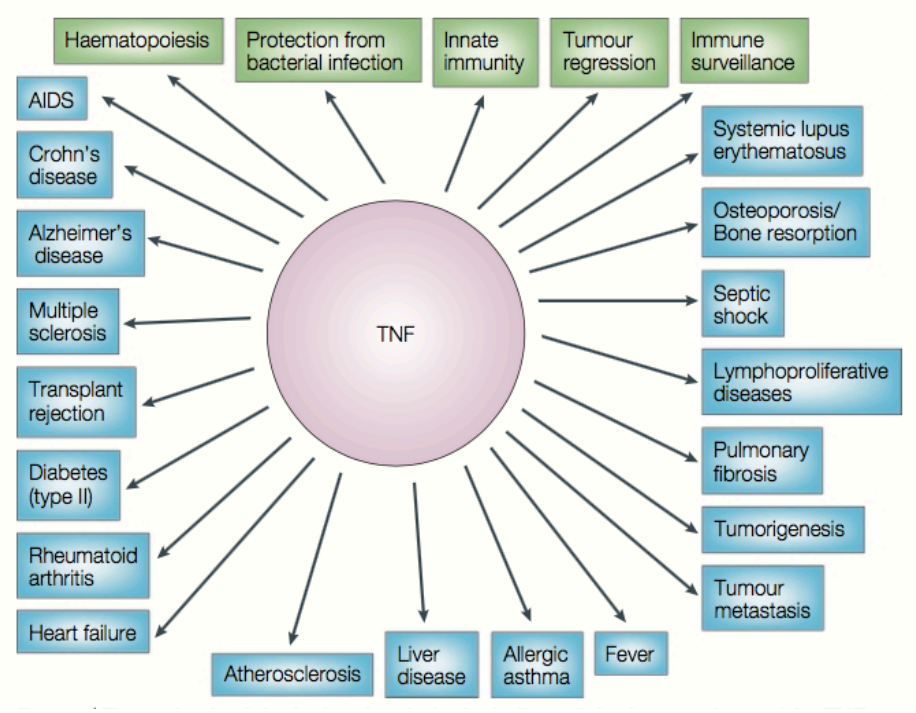


**Figure 1.1 | Compilation of the main effects caused by TNFα.** TNFα has important physiological roles (represented in green). However, it has been implicated in several diseases, (represented in blue) Image adapted from Bharat et al.[148].

## 1.1.1. TNFα expression and transport to the cell surface

Most of the host immune mechanisms are inducible, taking place upon infection, trauma, stress, which leads to release of a series of cytokines including TNFα, which alongside interleukin-1 (IL-1), acts at the apex of inflammation, triggering cytokine cascades.

Cytokines can be stored in cells ready for release, whereas others are transcribed *de novo* upon detection of an insult[5]. In the case of TNFα, the two processes have been described in a cell dependent manner, for example in macrophages it requires *de novo* transcription[7] whereas mast cells

store TNFα in granules, ready for release on demand[14]. In cells in which TNFα *de novo* transcription is required, it can be directly induced by immuno-globulin or complement receptor-mediated signalling or by pathogens through a variety of pattern recognition receptors (PRR) including Toll-like receptors (TLRs)[154,16]. For instance, lipopolysaccharide (LPS), which signals through TLR4, is a highly potent trigger of TNFα secretion[17]. LPS is a glycolipid that constitutes a major component of the membrane of gram-negative bacteria and can stimulate a variety of cells by initiating a signalling cascade that activates the inflammatory transcription factor NKκB, leading to transcription of inflammatory cytokines, including TNFα[17–20].

As TNFα is a glycosylated protein that is first translated in ribosomes attached to the endoplasmic reticulum (ER), generating a transmembrane TNFα precursor[21] (pro-TNFα), that appears to be retained in intracellular stores, specifically, the Golgi apparatus. TNFα is then transported to the plasma membrane, by incompletely understood processes that require its incorporation into vesicles [20] (Figure 1.2). Vesicular transport requires the sequential recruitment/release of a series of factors that promote vesicular budding, attachment to microtubules, recognition and fusion with specific membranes, thus ensuring that the secretory and membrane proteins that they transport are delivered to the appropriate cellular locations[22]. Factors promoting vesicular delivery from a donor to an accepter membrane include a specific network of proteins that in each case contain selected assortment of Rab proteins, molecular motors, tethers, N-ethylmaleimide-sensitive factor attachment receptors (SNARE) proteins and the regulators of all these factors[23].
TNFα secretion is a complex and controlled process and evidence suggests that it might be tailored to the cell type:
Granulocytes such as neutrophils, eosinophils and basophils or mast cells, store TNFα in granules. In basophils, TNFα trafficking pathway to the cell surface is not known[13]. In neutrophils, TNFα is stored within peroxidase-negative organelles, which are identified by their content of lactoferrin and gelatinase and are may be secondary or endosomal secretory vesicles. However, the mechanism of TNFα release in neutrophils has not been characterized in detail[24].
Eosinophils traffic TNFα through a tubulovesicular system and small secretory vesicles that bud from crystalloid granules and that serve to shuttle cytokines from the granules to the cell surface[25]. In mast cells, TNFα is released by classical degranulation that was shown by its rapid secretion during receptor-mediated exocytosis by cross-linking cell surface complexes IgE and Ag[14].

Finally, in macrophages, TNFα is packaged exclusively into a population of TGN-derived tubules/vesicles and it is constitutively secreted to plasma membrane[26,27]. However, the trafficking does not occur directly from the TGN to the cell surface. There are evidences that TNFα, after leaving the TGN, is delivered to intervening endosomes[28]. These are tubovesicular recycling endosomes.
Recycling endosomes are heterogeneous tubular-vesicular compartments with a single continuous membrane and luminal space occupying around 30% of cell volume[29]. Recycling endosomes

possesses various subdomains with different morphology, composition and function and displays a dynamic and intense trafficking activity exploiting the connection between the endocytic pathway and the exocytic pathway, recycling membrane components[30,31]. The recycling endosome participates in several important cellular mechanisms such as in epithelial cell-cell adhesion, cytoskeletal remodelling, cytokinesis or even in cell fate specification[32]. Cytokine secretion through the recycling endosome is not exclusive to macrophages. Microglial and NK cells represent another innate immune cell type in which TNFα use recycling endosomes to reach the cell surface[33].

In macrophages, the transport of TNFα through recycling endosome vesicles requires a set of specific SNAREs. The Q-SNARE complex is packaged with TNF-α into TGN-derived vesicles that upon reaching the recycling endosome, pairs with the resident R-SNARE VAMP3 fusing the TGN-derived vesicles with recycling endosome membranes [34].

Two Rab GTPases, Rab11 and Rab37, have been found to regulate surface delivery of TNFα in macrophages[35,26]. Rab11 is a well-known regulator of recycling endosome trafficking, and has been described to be required for the delivery of TNFα to the plasma membrane. Studies from the Stow lab showed a dependence of TNFα trafficking on Rab11 in macrophages: they compared TNFα levels at the cell surface using macrophages in which Rab11 was either permanently activated (constitutively active (CA)-Rab11) or permanently inactivated (dominant negative (DN)-Rab11). CA-Rab11 macrophages showed high expression of the transmembrane form of TNFα. Whereas cells bearing the DN-Rab11 failed to express the transmembrane form of TNFα (Figure 1.2)[35]. Other cytokines as IL-6 and IL-10 have been shown to use the same secretory pathway in macrophages[30].

Although it is important to emphasize that there is a only a handful of papers on TNF trafifkcing, and many of these from one research group, taken together, the evidence suggests that TNFα is trafficked in macrophages using the recycling endosome pathway, in particular using vesicles that are positive for Rab11 vesicles, a GTPase that is able to coordinate TNFα delivery to the cell surface. Figure 1.4 shows the proposed mechanisms by which TNFα and other cytokines are delivered to the surface in macrophages.

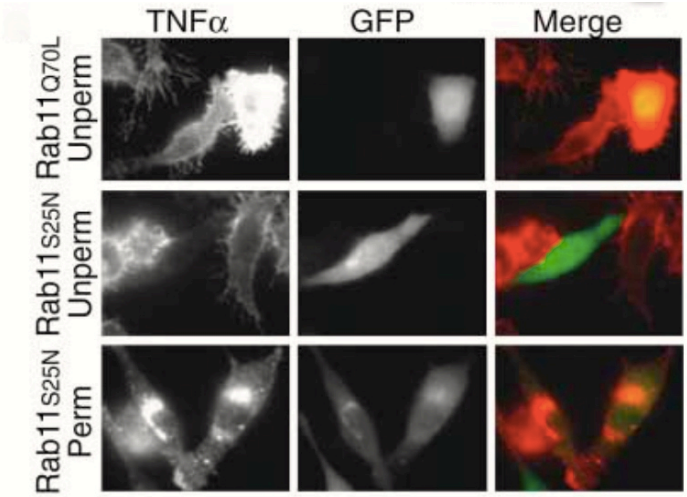


**Figure 1.2** | **Inter-dependence between Rab11 and TNFα surface delivery.** Cells are treated with LPS and TACE inhibitor (see below). $Rab11_{Q70L}$ cells that correspond to Rab11 constitutively active mutant, seem to increase the cell surface delivery of TNF-α. In contrast, $Rab11_{S25N,}$ the Rab11 dominant negative form, blocked TNF-α cell surface delivery without affecting newly synthesized TNF-α at the golgi complex as shown in permeabilized ($Rab11_{S25N}$ Perm) cells. Image adapted from Jennifer L. Stow et al., 2005.

### 1.1.2. TNFα release

Once incorporated into the cell surface, transmembrane TNFα is cleaved by a ADAM family metalloproteinase TNF-converting enzyme, TACE (as knows as ADAM17) at a site after alanine 76, thereby releasing the soluble active TNF-α [36,37,38]. The remaining transmembrane TNF-α is further processed by signal peptide peptidase-like 2b (SPPL2b) and it is translocated into the nucleus where it is involved in feedback loops that mediate the synthesis of new TNFα[39] (Figure 1.3).

In macrophages, TACE appears primarily in non-raft fractions and TNFα is delivered to lipid rafts or in phagocytic cups where TACE is in more abundance[127]. iRhom2 has been identified as key regulator of TACE transport to the plasma membrane; in the absence of iRhom2, TACE fails to exit the endoplasmic reticulum[40]. TACE is also regulated by LPS stimulation because LPS upregulates iRhom2 levels, permitting an increased TACE transport to the cell surface[40].

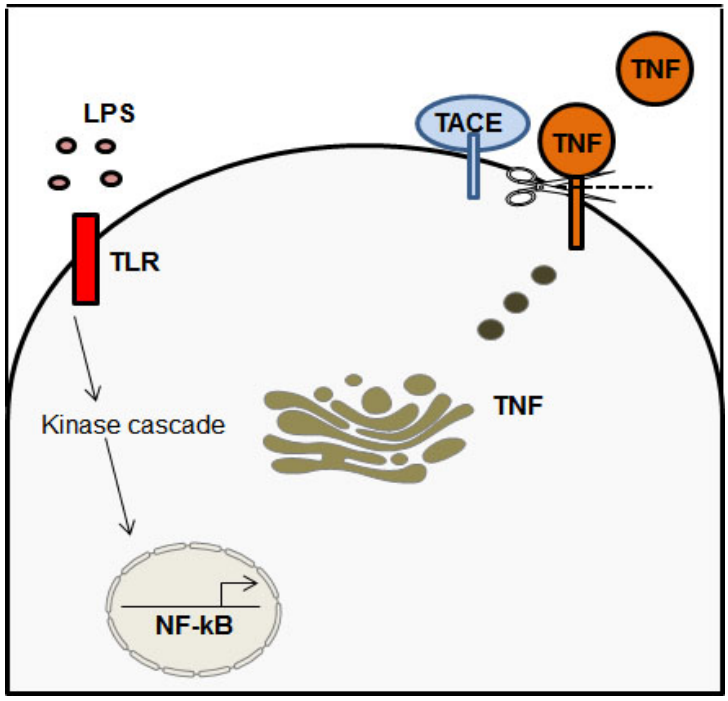


**Figure 1.3 | Biology of transmembrane TNFα and soluble TNFα.** LPS, which activates TLR4, leading to the transcriptional activity of NFkB, is highly potent inducer of TNFα production. Soluble TNFα is produced when TACE cleaves the transmembrane form of TNFα, allowing the release of a 17KDa portion.

## 1.2. Macrophages

Macrophages are the primary source of TNFα and key factors in innate immunity. These cells are evolutionary conserved phagocytes that evolved more than 500 milion years ago. They were first discovered in 19$^{th}$ century by Ilya Metchnikoff [41,42,43].

Macrophages are present in virtually all tissues. Until recently the origin of these tissue resident macrophages was believed to be circulating adult blood monocytes. However, recent publications have led to a paradigm shift demonstrating that many tissue macrophages are in fact established during embryonic development and persist into adulthood independently of blood monocytes[88,44].

Macrophages are key immune effector cells. These cells play homeostatic roles. They can clear, by phagocytosis, approximately 2 x $10^{11}$ erythrocytes each day which is an essential metabolic contribution to the survival of the host[45]. Macrophages are also involved in the removal of cellular debris and rapidly clear cells that have undergone apoptosis[46].

This clearance capacity is the basis underlying the ability of macrophages to identify endogenous danger signals. This function makes macrophages one of the primary sensors of danger in the host and that response is only one example of the many different stimuli that trigger macrophage activation in tissues[47,48].

Macrophages have an extraordinary plasticity which allows them to efficiently respond to environmental danger signals and change their phenotype by both innate and adaptive immune responses[49].

These cells are also the first line of defence against invading pathogens including bacteria, viruses, fungi and protozoa[50,51]. They are involved in the recognition, phagocytosis and destruction of microorganisms. Moreover, macrophages are also involved in antigen presentation and secretion of a wide variety of products including enzymes, complement components, coagulation factors, chemokines and cytokines[52].

Macrophages are very plastic, and perform different functions according to the cytokines they release. This plasticity has given rise to a controversial classification of macrophages in two types: M1 and M2 [53,54].

The M1 are grouped according to their ability to be activated and induce prototypic inflammatory responses producing several components as mentioned above. These are the type of macrophages most revelant to this thesis, because these are the macrophages that primarily produce TNFα [55].

The M2 designation includes basically all other types of macrophages and they include all macrophages that antagonize prototypic inflammatory responses. They are also involved in tissue remodelling, immunoregulation and allergy processes[56].

The controversy generated around this division is that not all macrophages display the characteristics of M1 or M2, as for example alveolar macrophages[53]. In addition, some scientists, believe that macrophages are sufficiently plastic to inter-convert into both types, but which hypothesis is correct requires validation [56].

Pro-inflammatory macrophages when activated by detection of pathogens or other danger signals, release cytokines such as TNF-α, IL-1, IL-6, IL-8, IL-12. These inflammatory cytokines recruit other immune cells that orchestrate the actions and fates of cells secreting them and those close by[57,58,59].

TNF-α, in macrophages, behaves as a powerful proinflammatory agent that regulates many functions. TNF-α is rapidly released upon some trauma, infection or exposure to LPS[17]. Moreover, IFN-γ-primed, LPS stimulated macrophages synthesize more TNF-α and secrete it faster than cells activated with LPS alone[60,61]. The pivotal role of TNF-α in macrophages is to orchestrate the production of a proinflammatory cytokine cascade[13]. Figure 1.4 show the trafficking model currently proposed for TNFα as well as IL-6 and IL-10, previously described for macrophages.

Of particular relevance for this thesis, macrophages are activated upon infection, including by viruses as influenza A viruses.

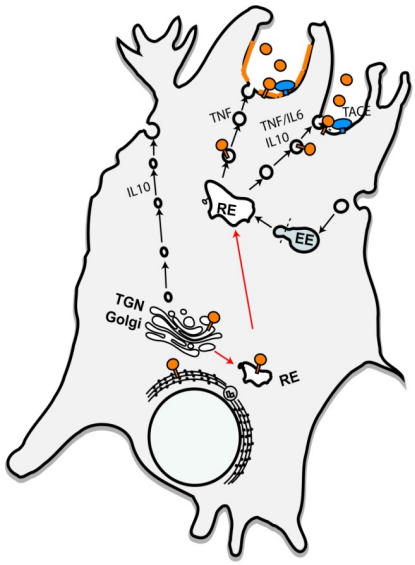


**Figure 1.4 | Model of cytokine secretion pathways in macrophages**. Representation of the pathway used by cytokines to be transported inside macrophages. IL-10 can be directly transported from TGN to the surface. However, cytokines as TNF and IL-6 use recycling endosome pathway to be transported until plasma membrane. Illustration by MJ Amorim.

## 1.3. Influenza Viruses – Impact of the disease

Commonly referred as flu, Influenza viruses are infectious agents that constitute an important disease in a large variety of vertebrates. It can be transmitted through aerosols, large droplets or direct contact with secretions. These viruses, in humans, are one of main causes of acute respiratory disease[62,63,64].

There are four types of influenza viruses: A, B, C and D; all are associated with human disease and provoke different levels of severity with exception of D that causes mild infections in pigs and cattle only[65].

Amongst Influenza viruses the type A is the most relevant to human health and it is responsible for seasonal epidemics and periodic pandemics that lead to substantial human mortality and morbidity and a considerable financial burden worldwide every year[66.67].

Influenza A virus (IAV) contains a single and negative strand RNA genome of 13 kb that is split into 8 different segments. Besides humans, it infects a variety of hosts including pigs, horses, bats and wild birds, which are the primary reservoir of most subtypes of IAV[68]. Because of this wide host range, and an encoded error prone polymerase that induces high mutation rates, influenza A viruses are genetically very diverse, subtyped according to the hemagglutinin (H or HA) and neuraminidase (N or NA) viral surface proteins[69].

In total, there are eighteen different hemagglutinins identified (H1-H18) and eleven neuraminidase subtypes that are scattered through a wide range of hosts. Viruses are species specific as a result of

adaptation to that host cellular environment for optimal growth. In humans, for example yearly currently circulating epidemic strains belong to H3N2 and H1N1 subtypes. On average, yearly epidemics result in three to five million cases of severe illness and 250.000 to 500.000 associated deaths [70].

Occasionally, IAV manages to jump the host species barrier and establish a productive infection in humans originating IAV pandemic outbreaks associated with severe outcomes. [71]. Factors that drive viral evolution and hence adaptation to different niches, include antigenic drifts and antigenic shifts[72]. The first occurs in both influenza A and influenza B viruses and results from an error prone viral polymerase that induces accumulation of mutations in HA and NA. As a consequence viral antigens change allowing the virus to spread throughout a partially immune population[73].

Antigenic shift occurs when the same cell is co-infected with two different strains, mixing viral genomes through a process called genome reassortment. These viruses might contain a new combination of HA and NA present in the surface of the virion and remainder segments adapted to replicate in humans [74]. When reassortment takes place, the immune system of the host is unable to recognise the novel viral strain as the defences previously developed against NA and HA are no longer useful[75].

The unpredictability of IAV evolution and interspecies movement creates continual public health challenges. [76].

IAV outbreaks of this sort of a variety of origins occurred during recent history with variable severity (Figure 1.5). These outbreaks include the well-known pandemics that gave rise to seasonal epidemics thereafter known as Spanish flu in 1918 that killed over 40 million people worldwide[70], the Asian Flu in 1957, the 1968 Hong Kong Flu and the 2009 Swine Flu. It also includes sporadic incursions of viruses, such as the avian strains H5N1 and H7N9 resulting in high mortality of infected people. These infections have so far not been able to spread in humans, but had a global effect in creating awareness to potential pandemics.

Influenza B viruses also contributes to the burden of seasonal epidemics and both influenza A and B are considered during annual vaccine design. In case of influenza B, mutagenesis rate in antigenic proteins is lower[77]. Consequently, antigenic drifts have a much less significant role in flu epidemics. The host range of influenza B is restricted to human and seals. However, the number of cases of influenza B in humans is inferior to those caused by influenza A[78] (Figure 1.6)

Influenza C viruses are known to cause infrequent mild infections in humans and pigs and it. The impact of this infections is very low, and this type is not considered during vaccine design[79].

Even though there is extensive development of antiviral drugs and yearly updated vaccination, influenza viruses continue to cause epidemics and periodic pandemics with severe outcomes. Therefore, novel antivirals are needed that might be identified through the understanding of how the virus interacts with the host cell upon infection.

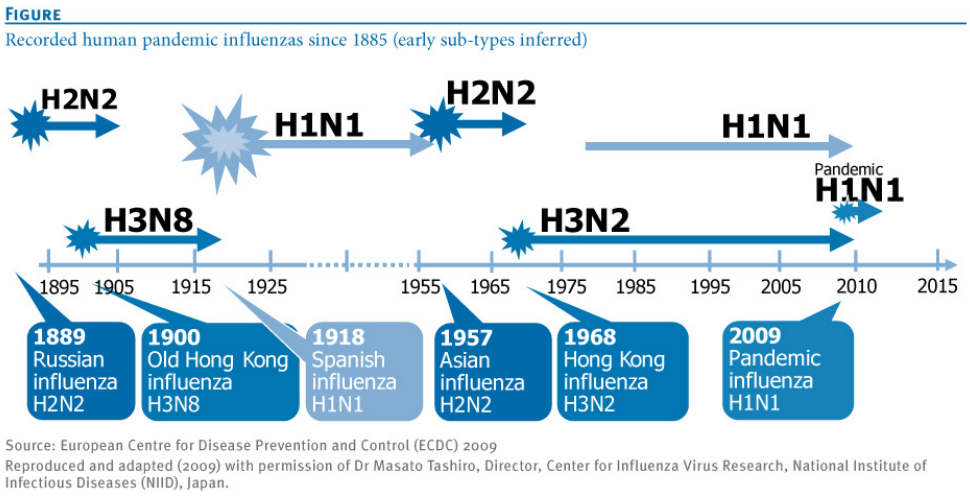


**Figure 1.5** | Representation of IAV outbreaks occurred during recent history. Data acquired from ECDC (2009).

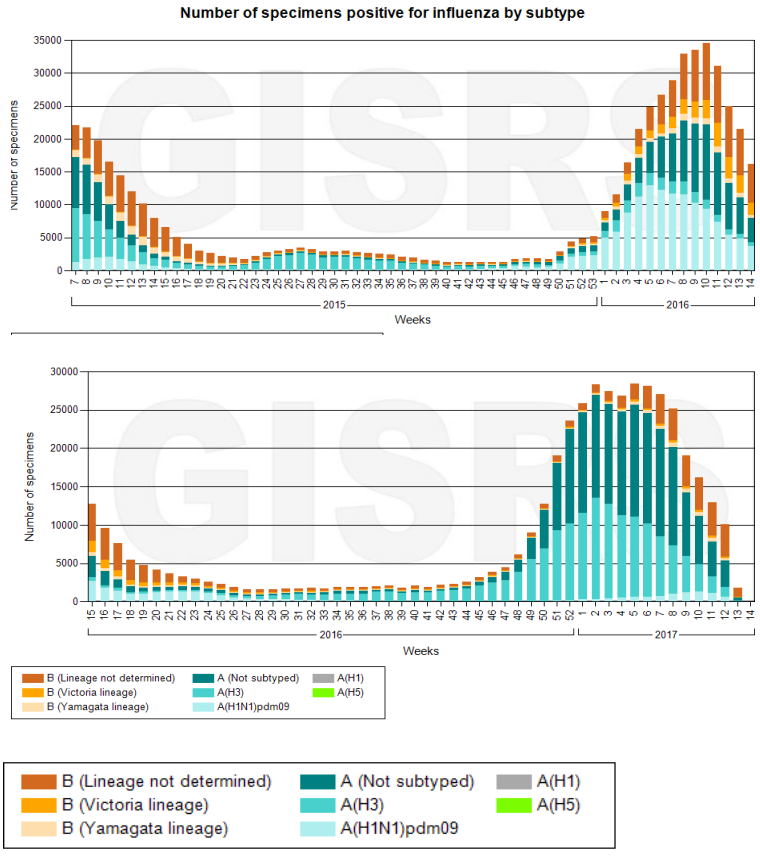


**Figure 1.6** / **Number of specimens positive for influenza by subtype.** Number and subtypes of influenza specimens circulating worldwide during winter season 2015-17. Data acquired from WHO website.

### 1.3.1. Influenza A - Virion

Isolated for the first time in 1933[80] , IAV are enveloped viruses, members of the *Orthomyxoviridae* family. Its genome is unusual, formed by eight single-stranded negative-sense viral RNA (vRNA) segments. All segments share the same organization with the middle coding region flanked by two small untranslated regions which are highly conserved and partially complementar[80]. These dsRNA structures work as a docking platforms for the heterotrimeric viral polymerase and the remaining sequence is bound by multiple copies of nucleoprotein (NP), and this constitutes the viral ribonucleoprotein complex (vRNP) (Figure 1.7 B)[81]. The heterotrimeric viral RNA polymerase complex is formed by polymerase acidic (PA), polymerase basic 1 (PB1) and polymerase basic 2 (PB2) proteins. Inside the virion, vRNPs are arranged in a 7+1 conformation[82,83]. The viral envelope surrounding vRNPs is derived from the host lipid bilayer and it contains three viral transmembrane proteins which are hemagglutinin (HA), neuraminidase (NA) and matrix protein 2 (M2)[84]. The inner core of the viral particle encloses matrix protein 1 (M1), and non-structural protein 2 (NS2)[85,86] and the viral genome (Figure 1.7 A). The eight segments encode nine essential proteins and several accessory proteins up to 17 identified so far whose expression is cell-type and strain dependent. Table 1.1 shows the expression of all viral proteins for A/Puerto Rico/8/1934 (PR8) H1N1, the wild-type influenza A model used in our laboratory.

Other proteins as M3[87],PA-N155[88], PA-N182[88] or PB1-F2[81] have been identified, but their role during infection requires characterization.

**Table 1.1: Genome segments and functions of coded peptides of H1N1 influenza A virus PR8**

| Gene ID | Protein | Main function | Symbol | Protein length (aa) |
|---|---|---|---|---|
| **1** | Polymerase basic subunit 2 | 5'-cap recognition | **PB2** | 759 |
| **2** | Polymerase basic subunit 1 | RNA-dependent RNA polymerase<br>Mitochondrial targeting | **PB1** | 757 |
| **3** | Polymerase acidic protein | 5'-cap endonuclease | **PA** | 716 |
| | Protein PA-X (auxiliary protein) | Repression of RNApoII gene expression | **PA-X** | 252 |
| | Protein PB1-F2 (auxiliary protein) | Pro-apoptotic activity | **PB1-F2** | 87 |
| | Protein PA-N182 | Undefined function | **PA-N182** | - |
| | Protein PB1-S1 | Undefined function | **PB1-S1** | - |
| | Protein PA-N155 | Undefined function | **PA-N155** | - |
| **4** | Hemagglutinin | Binding to surface receptors<br>Endosomal function | **HA** | 565 |
| **5** | Nucleoprotein | Coating, nuclear export and replication | **NP** | 498 |
| **6** | Neuraminidase | Cleavage of HA-receptor binding | **NA** | 454 |
| **7** | Matrix protein 1 | Nuclear export of vRNPs<br>Viral budding | **M1** | 252 |
| | Matrix protein 2 | vRNPs release | **M2** | 97 |
| | Matrix 42 (auxiliary protein) | Replaces M2 in adamantine containing media | **M42** | 97 |
| | Matrix protein 3 | Undefined function | **M3** | - |
| **8** | Non-structural protein 1 | Inhibition of interferon response and nuclear export | **NS1** | 230 |
| | Nuclear export protein or Non-structural protein 2 | vRNP nuclear export, along with M1 and NP | **NEP or NS2** | 121 |

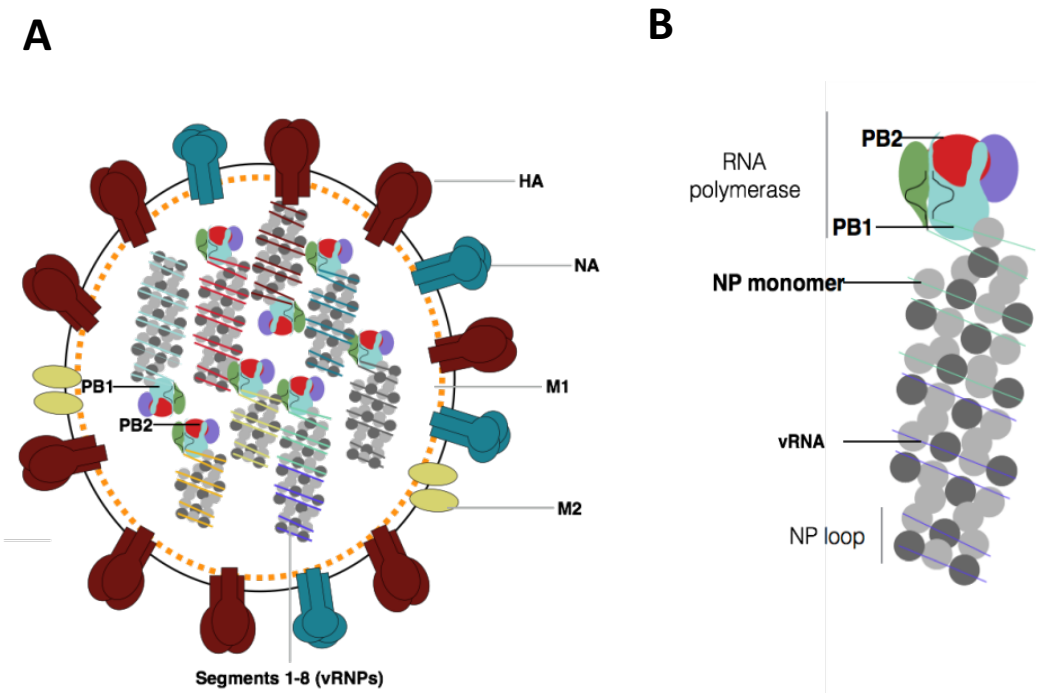


**Figure 1.7 | Influenza A virus. a)** Virion. The viral particle has an envelope derived from the host lipid bilayer with surface proteins HA, NA and M2. The inner core contains the segmented genome: eight segments consisting of negative-sense RNA with NP and the viral polymerase complex. **b)** vRNP complex. vRNP bind NP stoichiometrically. The extremities are complementary and form a double-stranded structure bound by the polymerase complex PA, PB1 and PB2. Illustration by MJ Amorim.

### 1.3.2. Influenza A virus – Replication Cycle

Viral infection is initiated when a virion binds to cell surface receptors that contain sialic acid, followed by endocytosis of the virion[89].

Following internalization and pH drop through endosome maturation, HA suffers a conformational changes which leads to the fusion of the virion and endosomal membranes providing a portal of access to the cytoplasm of the cell host[90].

Then, vRNPs are released from endosomes and transported into the nucleus to be transcribed and replicated [91]. The transcribed mRNAs are exported to the cytoplasm and translated into proteins by cellular ribosomes. Newly translated viral proteins are transported to the nucleus (PB1, PB2, NP, M1 and NEP) or the plasma membrane (HA, NA and M2). After nuclear entry of those proteins the production of progeny vRNPs ensues. Newly synthesised vRNPs are then exported to the cytoplasm and transported to the plasma membrane to be incorporated into viral particles that bud and are released from the cell (Figure 1.8)[92,93].

The IAV lifecycle can be divided into the following sections detailed below: 1) viral entry, disassembly, nuclear export; 2) viral transcription and replication; 3) viral assembly, budding and release.

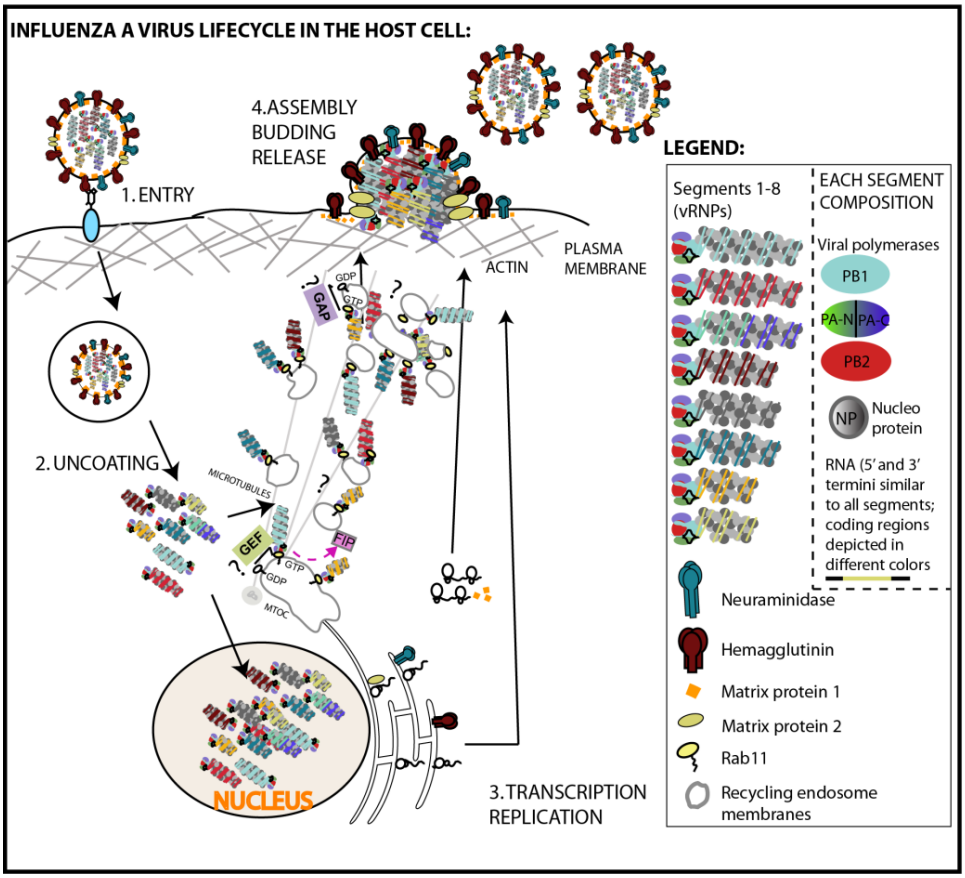


**Figure 1.8 | Influenza A virus replication cycle.** IAV enters cells by endocytosis after binding of the viral protein HA to sialic acid residues at the plasma membrane. Following internalization, endosomal acidification results in the fusion between the virion and endosomal membranes. Then vRNPs are released to the cytoplasm towards the nucleus when transcription and replication occurs. The new segments are exported to the cytoplasm. vRNPs accumulate near to MTOC, loaded onto Rab11 vesicles and are transported by recycling endosome to the assembly sites at the plasma membrane. Each segment is then incorporated into a budding particle created with host membranes. Illustration by MJ Amorim.

### 1.3.3. Viral entry, disassembly and nuclear import

IAV enters cells in an endosome after the viral protein HA binds to host receptor molecules[94]. HA is a homotrimer that forms spikes on the viral lipid membrane. These spikes of HA bind to sialic acids which are found on the surface of the host cell's membrane[95]. The HA precursor, HA0, is made up of two subunits: HA1, which contains the receptor binding domain, and HA2, which contains the fusion peptide[39]. Those subunits are linked by disulphide bonds. There are two major linkages between sialic acids and the carbohydrates which are bound in glycoproteins: $\alpha(2,3)$ and $\alpha(2,6)$. These linkages are extremely important for the specificity of de HA molecules in binding to cell surface sialic acid receptors found in different species[96].

Upon binding to the host cell's sialic acid residues, receptor-mediated endocytosis occurs and the virus enters the host cell in an endosome. During this process, the virus is transported from early to late endosomes, in actin and microtubule-dependent manner[89,97].

As endosome matures, the pH drops causing a conformational change in HA which triggers the fusion of the viral and endosomal membranes[98]. The acidic environment of the endosome is not only important for inducing the conformation of HA but also opens up the M2 ion channel, which is a transmembrane protein of the virus that forms tetramers, whose membrane domains form a channel that acts as a proton-selective ion channel[99,100]. Opening the M2 ion channels acidifies the virus inner core weakening the affinity between matrix protein M1 and vRNPs. Thus, vRNPs are free to enter the host cell's cytoplasm and they are then transported into the nucleus through the nuclear pore complex (NPC) in order to undergo transcription and replication[101,102].

### 1.3.4. Genome transcription and replication

After nuclear import, influenza vRNPs are transcribed to produce viral mRNAs (known as primary transcription) in a process that is independent of *de novo* viral protein synthesis[69].

Transcription is performed by the viral RNA dependent RNA polymerase (RdRp)[103]. The viral RdRp contain three viral proteins: PB1, PB2 and PA. PB2 binds to the 5´ methylated caps of cellular mRNAs and present these mRNAs to subunit PA that cleaves the cellular mRNAs 10-13 nucleotides downstream, in a mechanism named "cap-snatching"[104,105]. This cellular capped RNA fragment is used by the viral RdRp to prime viral transcription[106].

Once the caps are acquired, mRNAs are generated by transcription from a vRNP template using the viral polymerase complex on the vRNP. Transcription is terminated through the creation of a poly-A tail, produced by reiterative shuttering and copying of the poly-U sequence motif at the conserved 5'end to the vRNA[107].

After primary transcription, viral mRNAs are exported to the cytoplasm and translated by cellular ribosomes. Some viral proteins, required to produce the vRNP complex are subsequently imported into the nucleus, and viral replication starts[108]. The influenza viral genome is made up of negative strands of RNA. In order for genome to be transcribed, it first must be converted into a positive sense RNA, called (cRNA), that serve as a template for the production of viral RNAs for amplification of vRNA and generation of progeny vRNPs[109,110].

The formation of both cRNA and progeny vRNPs, requires newly translated NP and polymerase complex proteins to coat the RNA and include the viral polymerase[111].

Newly synthesised progeny vRNPs must be transported from the nucleus to viral assembly sites located at the plasma membrane. The first step in this process is nuclear export of vRNPs[112].

vRNPs associate with components of the CRM1 (also known as exportin-1) in a daisy-chain as follows. CRM1 protein is a nuclear export receptor that recognizes cargo proteins that have leucine-rich nuclear export signals (NESs)[113]. CRM1 binds to NESs motifs in cargo proteins in the nucleus in

association with the GTP-loaded RAN GTPase to leave the nucleus across the NPC[114]. vRNPs bind to CRM1-RAN-GTP complexes via 'daisy chain' complex with M1 and NEP viral proteins (vRNP-M1-NEP)[115]. In the cytosolic side of the NPC, the RAN GTPase-activating protein (RANGAP) hydrolyses RAN-GTP to RNA-GDP and this process facilitates dissociation of the viral complex that is release into the cytoplasm[81,116].

### 1.3.5. Viral assembly, budding and release

Nuclear export is only a part of the process of transporting vRNPs to the IAV budding site. vRNPs must navigate through a dense cytoplasm to reach the plasma membrane where the viral particle assembles and buds out of the cell[117].

After nuclear export, vRNPs accumulate near the microtubule organizing centre (MTOC), which is located adjacent to the nucleus[118,119]. Later, vRNPs align with the microtubule network on route to the plasma membrane[120]. This alignment is performed when vRNPs interact with recycling endosomes via the small GTPase Rab11-GTP which is to the regulator of the trafficking of the recycling endosome[121,122].

Overexpression of a dominant-negative Rab11 mutant protein impairs the association of vRNPs with Rab11-positive vesicles, disrupting the accumulation of vRNPs at the plasma membrane and reducing the output of infectious progeny virus[123,124].

Our group obtained evidence that vRNPs binding to Rab11a vesicles competes with cognate binding partners of Rab11, for example, the family of proteins called Rab11-family-interacting proteins (abbreviation?). As a consequence, the recycling endosome pathway becomes impaired in infected cells (Figure 1.9)[125]. This mechanism leads to vesicular clustering of vesicles carrying different vRNPs throughout the cytoplasm. Although not supported by compelling experimental evidence, it is possible that vesicular clustering is necessary for viral assembly as it places the pool of 8 distinct vRNPs in close contact, permitting the formation of the viral genome[119] . As noted above, the trafficking of TNF also depends on the recycling endosome. Hence although not yet explored, impairment of the recycling endosome is predicted to have additional consequences to the host cell, impairing the transport of host factors to the plasma membrane, including cytokines such as TNFα in macrophages.

Viral assembly at the plasma membrane occurs at domains called lipid rafts. Envelope proteins HA and NA are targeted to those structures, whose lipid content and biophysical properties provide a local alteration in membrane curvature that facilitates the budding process[86,126,127].

Cytoplasmic tails of HA and NA serve as docking sites for M1 and binding of vRNPs to the budding site[128]. M2 protein flanks lipid rafts and is involved in membrane scission to release the virion After this process the virion is still coupled to the cell membrane due to the interaction of HA with sialic acid[86,129]. NA cleaves this HA-sialic acid bond releasing the virion[130]. After particle release, the viral protein HA is cleaved by extracellular proteases. This modification is essential for membrane fusion in the next round of infection[131].

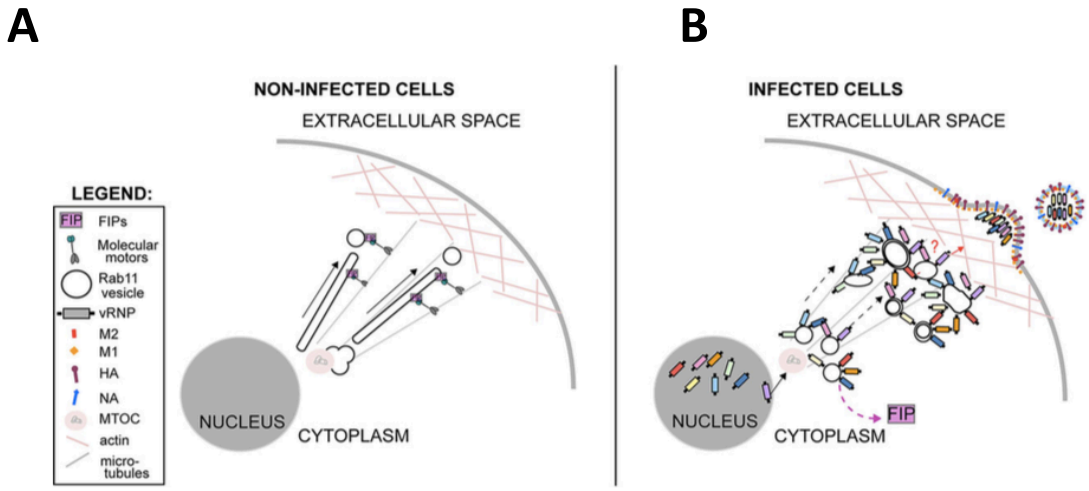


**Figure 1.9 | vRNP outcompete FIPs by Rab11 vesicles causing impairment in recycling endosome**. **A)** In non-infected cells, Rab11 binds to FIPs allowing transport of these vesicles by molecular motors along the microtubule network. In contrast in **B)** infected cells, vRNPs outcompete FIPs resulting in the cytoplasmic accumulation of vRNP containing vesicles. This competition leads to a reduction in the levels of Rab11 effectors impairing the recycling process. Illustration by MJ Amorim.

### 1.3.6. Host immune responses to IAV

When IAV invades the host, the first barrier it encounters is the mucus layer covering the respiratory and oral epithelia. Overcoming this barrier, it can bind the respiratory epithelial cells, be internalized and start replication[130].

Upon IAV penetration in the cells, the cellular defense mechanisms are activated. Alveolar epithelial cells are equipped with receptors to sense the presence of viral RNA and trigger the cellular signalling pathways to clear viral infection[132]. These cellular receptors are pattern-recognition receptors (PRRs)[131].

Three major families of PRRs have been identified: the transmembrane Toll-like receptors (TLR), the cytosolic retinoic acid-inducible gene-I (RIG-I)-like receptors (RLR) and Nod-like receptors (NLRs)[133,134]. NLRs are cytosolic and form a multiprotein inflammasome complex that provokes modifications in procaspase I, contributing to the production of active forms of IL-1β and IL-18 in various cells such as neutrophils, monocytes and macrophages[135]. TLRs are the major group of transmembrane receptors that are involved in the detection of viral nucleic acids. TLRs bind with the ssRNA and dsRNA derived from IAV activating the production of pro-inflammatory cytokines as well as IFN signalling pathways[133]. Whereas, RIG-I receptor has an important role in recognizes vRNP and transcriptional intermediates that contain 5'-triphosphate produced during the viral replication[134] and detects, intracellularly, Influenza viral ssRNA. That way, RIG-I initiates conformational changes to expose caspase activation and it recruits domains (CARDs) that are ubiquitinated by the action of E3

ligases as TRIM25. Then, RIG-I is associated with mitochondrial antiviral signalling adaptor (MAVS) and it leads to the activation of NF-κB and IFN type I.

The viral recognition by host sensors lead to activation of subsequent signalling that results in the secretion of inflammatory cytokines such as IL-6, IL-8, IFNs and TNFα, the studied cytokine in this work, creating an anti-viral state[132]. The secretion of proinflammatory cytokines contributes to the modulation of T cells response as well as to the recruitment of different immune cells such as monocytes, neutrophils and macrophages[138,139]. In fact, macrophages are very crucial at this point because these cells produce higher levels of TNFα and nitric oxide synthase (NOS2) leading to the IAV-induced pathologic response[136].

Many reports show the importance of TNFα in IAV infection[135,136]. For instance, a report demonstrated that soluble TNFα is required to restrain the immune response and the magnitude of injury in mice infected with IAV[137].

All viruses have developed strategies to counteract host immunity. IAV is no exception and has evolved strategies to escape the immune responses in order to gain space for its replication and progeny within their hosts. IAV uses several mechanisms to fight against the innate immune system of host.

The principal mechanisms occur through NS1 protein, polymerase complexes, PB1-F2 and PA-X and M2 protein[132]. NS1 viral protein is the most important factor for the innate immune inhibition. This protein is involved in inhibition of IFN-mediated immune responses, once NS1 contains RNA binding domains that can bind with viral RNA and prevent its recognition by TLRs and RIG-I by supressing E3 ligase TRIM25 which is required for posttranslational modification of RIG-I[138]. Moreover, NS1 protein causes impairment in the processing of cellular mRNA in the nucleus which will prevents efficient IFN expression. Viral proteins as PB1, PB2 and PA are also involved in the viral ability to escape host immune responses. These proteins as mentioned synthesise viral progeny RNA, cRNA and mRNA and because viral transcription requires ain the cap-snatching of host mRNAs, the levels of host mRNAs are reduced in the host cell preventing the expression of many genes including IFN-β[106]. In addition, M2 protein has been identified to prevent the activation of TLRs because this protein interferes with cellular autophagy which is directly related with TLR activation during viral infection[139].

Identifying the mechanisms, the virus uses to fight host immunity is important for human health. Mechanisms depend on the viral type and strain. For example, H3N2 types are generally more virulent than H1N1 in humans[66]. Identifying viral signatures responsible for specific immune targeting processes might be used to mitigate severity of the disease and lead to novel therapies.

## 1.4. Objectives of the work

TNF-α is a cytokine produced by several types of cells and it plays fundamental roles in the healthy and diseased organism. Macrophages are the primary producers of TNFα upon injury, and its secretion contributes to the induction of a pro-inflammatory state necessary to resolve the assault. In activated macrophages, TNFα is transcribed *de novo*, translated in ribosomes attached the ER and secreted using specific arms of the secretory pathway. It was reported that in this system, TNF-α was transported to the cell surface using the recycling endosome pathway and requiring the small GTPase Rab11[35].

Influenza A virus are important human pathogens causing excess mortality. As any other virus IAV must use the host machinery for an efficient replication. IAV was shown to use the recycling endosome to transport progeny RNAs (vRNPs) to the surface, requiring the small GTPase Rab11. However, vRNP binding to Rab11-vesicles causes alterations to the pathway, impairing the flow of vesicles and originating vesicular clustering.

IAV escapes host immunity in a variety of ways[132,140]. In this work we aim to understand if viral induced impairment of the recycling pathway could affect release of TNFα in macrophages (Figure 1.10).

This thesis is divided into two main chapters of results in which we have investigated:

I. Whether a series of IAV strains replicate in macrophages and require the recycling endosome to transport vRNPs to sites of viral assembly;
II. The role of Rab11 in TNF-α transport in macrophages and alterations in TNF-α secretion upon IAV infection.

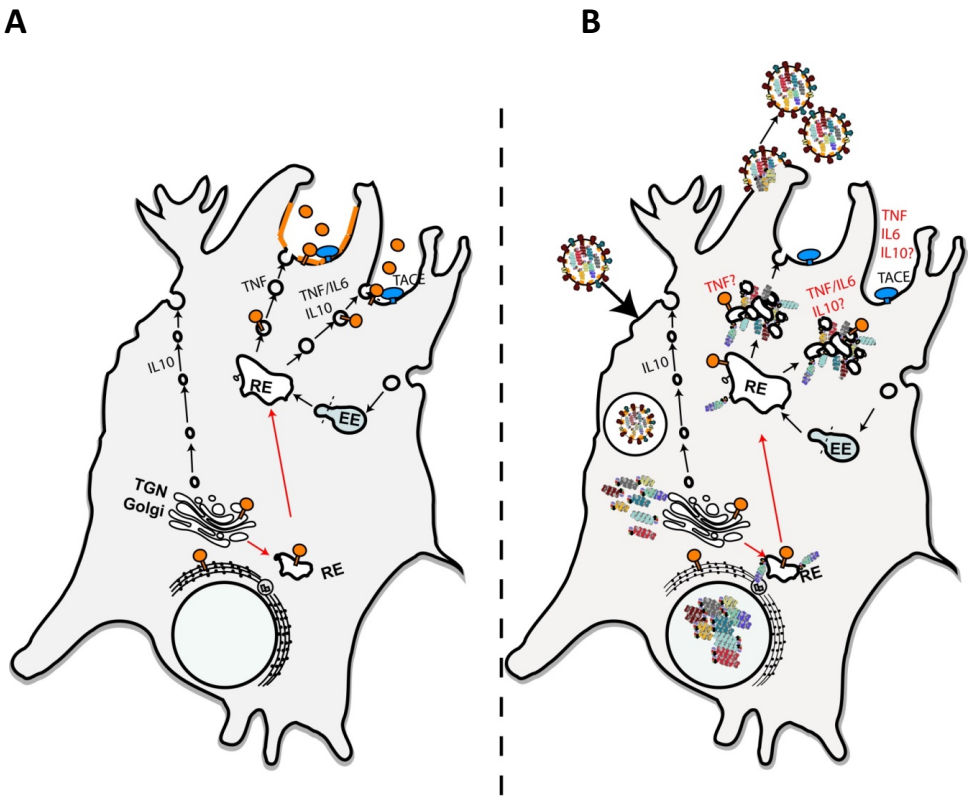


**Figure 1.10 | Model for the trafficking of cytokines to the cell surface in macrophages and how IAV could negatively influence this transport.** A) Pathways used for the transport of cytokines inside macrophages. IL-10 can be directly transported from TGN to the surface. However, cytokines such as TNFα and IL-6 use recycling endosome vesicles to be delivered to the cell surface B) Models for potential IAV interference with pathways used by macrophages to deliver cytokines to the surface. Cytokine release in macrophages and how this Pathways affected IAV infection causes impairment in recycling endosome flow Illustration by MJ Amorim.

## 2. Materials and methods

**Cell Lines |** Three different cell lines were used throughout this work according to specific requirements.

1) HeLa cells originated from cervical adenocarcinogenic epithelia were used to characterize TNFα expression upon transfection.
2) Madin-Darby canine kidney epithelial cells (MDCK) were used in viral titration assays by plaque formation, due to their high adherence to the substrate and resistance to the presence of trypsin.
3) RAW264.7 semi-adherent macrophages cells from mouse were used as a model of IAV infection in macrophages and to assess the expression and secretion of TNFα.

**Stable Cell Lines |** HeLa and RAW264.7 cells were transduced individually with lentivirus encoding GFP tagged Rab11a WT and Rab11a containing the point mutation S25N, that renders the protein inactive (dominant negative (DN)). These stable cell lines will be henceforward addressed as "GFP-Rab11 WT" and "GFP-Rab11 DN", respectively.

**Cell culture |** HeLa and MDCK cells were cultured in Dulbecco Modified Eagle medium (DMEM) (Life technologies), supplemented with 10% fetal bovine serum (v/v), 200mM glutamine, 100U/mL penicillin and 10μm/mL streptomycin. RAW264.7 cells were cultured in Dulbecco Modified Eagle medium (DMEM) high glucose with L-glutamine and sodium pyruvate (Biowest) supplemented with 10% fetal bovine serum (V/V), 100U/mL penicillin and 10μm/mL streptomycin. Stable cell lines described above were also supplemented with 1.25 μg/mL puromycin. For specific purposes, cells were incubated with 1μM LPS (R&D Systems) during 2 hours and/or 15μM TACE inhibitor (table 2.1) during 1 hour before processing. All cells were grown at 37°C in a humidified atmosphere containing 5% $CO_2$.

**Infection |** Infections were carried out with reverse genetics-derived A/Puerto Rico/8/34 (PR8; H1N1) and PR8 ΔNS1 grown in MDCK with exception of X31 that were grown in chicken eggs. Viruses will be described in chapter 3.
The viruses were added at a multiplicity of infection (MOI) of three in each case in serum-free DMEM (Biowest). After 45 minutes of infection, cells were overlaid with serum-free DMEM supplemented with 0.14% (w/v) bovine serum albumin (BSA) or complete DMEM.

**Plasmid transfection |** $10^5$ HeLa cells were transfected with 500ng of TNFα plasmid using Lipofectamine® LXT, according to the manufacturer's instructions (Table 2.1) and incubated for 24h prior to any further treatment, processing or analyses.

**RNA extraction |** Quick spin column purification of total RNA directly from TRIzol® was performed accordingly to manufacturer's instructions using Direct-Zol™ RNA MiniPrep Kit from Zymo Research.

**cDNA synthesis |** cDNA was obtained upon RNA extraction through a Reverse Transcription reaction accordingly to NZY First-Strand cDNA Synthesis kit from NZYTech.

**RT-qPCR |** Quantification of gene expression of specific genes was obtained with iTaq™ Universal SYBR® Green Supermix from BioRad. Forward and reverse primers (4μM) indicated in table 2.1 were used to amplify the gene of interest and actin as a control. Standard DNA dilutions (1:4) were made using a mix of the GFP-Rab11 WT plus LPS sample. Real-Time gene expression was measured using CFX 384 Touch™ Real-Time PCR system from BioRad as follows: 10 minutes at 95°C, 40 cycles consisting of 15 seconds at 95°C and 1 minute at 60°C. Each condition was normalized to its actin sample values.

**Plaque assay |** In order to quantify virus titers, a confluent monolayer of MDCK cells was infected with 1:10 serial dilutions of each supernatant sample ($10^{-1}$ to $10^{-6}$) in serum free media containing 4% Avicel, 0.14% BSA, 1μg/mL TPCK trypsin and cells were kept at the previous conditions for 36 hours. At this time, cells were fixed and stained using 4% PFA – 0.2% toluidine blue solution. Plaque forming units were then counted for each dilution and viral titers were calculated.

**Western blot |** Upon harvest, cell samples were kept in Laemmli buffer at -20°C. Proteins were separated by electrophoresis in a 17.5% polyacrylamide gels and transferred to a nitrocellulose membrane at 200mA for 45 minutes using filter papers soaked in two sets of buffers: starting at the negative pole, 3 layers of filter paper soaked in 0.3M Tris and 20% (v/v) ethanol followed by 3 layers of 25mM Tris and 20% ethanol (v/v) were laid below the nitrocellulose membrane. Then, the acrylamide gel was placed over the membrane, followed by another 6 layers of filter paper in 25mM Tris and 20% (v/v) ethanol, under the positive pole. Upon transfer, membranes were incubated with primary antibodies against the proteins of interest overnight at 4°C, followed by extensive washing in PBST. Membranes were then incubated with host-specific secondary antibodies conjugated to fluorochromes LiCor 800 and/or 680 for 45 minutes at room temperature and washed three times in PBST followed 10 minutes in PBS. (Table 2.1). Membranes were scanned using LiCor Biosciences Odyssey near-infrared platform.

**Protein precipitation |** Supernatants were precipitated mixing 500μL methanol and 125μL chloroform with 500μL of sample by vortexing. The mixture was centrifuged at 300G for 5 minutes and the upper organic phase discarded. Then, samples were mixed with 600μL methanol and centrifuged as referred before. After that, the pellet was dissolved in 100μL *Lammeli's* sample buffer.

**Immunofluorescence |** Raw264.7 and stable cell lines were seeded on glass coverslips with 13mm of size (TRADE) and then infected. After 8 hours and 16 hours post-infection cells were fixed in 4% (V/V) paraformaldehyde for 20 minutes at 37°C then washed in 1% (w/v) NCS-PBS and

permeabilised in 0.2% Trition X-100-PBS for 7 minutes. Blocking and washing steps between each procedure were performed using 1% (v/v) NCS-PBS. Primary antibodies staining was performed against proteins of interest for 1 hour followed by secondary staining using host-specific conjugated antibodies Alexa 488, 647 or 568 incubated in the dark for 45 minutes at room temperature (table 2.1). The cell nucleus was stained using Hoechst incubated with the secondary antibodies at dilution of 1:1000. Coverslips were mounted using Dako© mounting media. Confocal images were acquired on a Leica SP5 confocal using a 63x 1.40-0.60NA oil immersion objective illuminated with Diode, Argon, DPSS 561 and HeNe 633 lasers.

**Measurement of vesicular area |** Confocal images stained with NP and Rab11 were analysed using Fiji 'vesicle size' plugin. The output value of the area of each vesicle was used to calculated the frequency distribution within the three size categories of the areas (in $\mu m^2$): 0-15 – small; 0.15-0-30 – medium; > 0.30 – large. An average between 15 to 30 cells were analyzed per condition.

**Co-localisation analysis |** Confocal images were analyzed using Fiji plugin 'Colocalization threshold', to determine the overlap between indicated stainings. The output value of Pearson's Correlation Coefficient was acquired for ten cells per condition.

**ELISA |** Detection of TNFα in culture supernatants of RAW264.7 and stable cell lines was performed by ELISA according to manufacturer's instruction (Mouse TNF-alpha Quantikine ELISA kit from R&D system®). 50μL of Assay diluent were added to wells of microtiter plates. Samples (50μL) were loaded in duplicate and incubated for 2 hours at room temperature, followed by the addition of 100μL of Mouse TNFα Conjugate antibody. After 2 hours, 100μL of Substrate solution were added to each well for 30 minutes at room temperature. The reaction was stopped with 100μL of Stop solution. Plates were read in Victor 3 1420-012 at 450nm with values at 570nm subtracted. Plates were washed five times with washing buffer after each step. As reference for quantification, a standard curve was established by a serial dilution of Mouse TNFα Standard provided and generated using the four parameter logistic (4-PL) curve-fit.

**FACS |** Raw264.7 macrophages were infected or mock-infected and stimulated with LPS for 2 hours and/or incubated with TACE inhibitor for 1 hour. After 16h p.i., cells were fixed with 4% PFA incubated with Fc-block solution for 15 minutes at 4°C, washed and cell surface was labelled with TNFα antibody for 30 minutes at 4°C, in dark. Cells were washed twice with ice-cold FACS Buffer (containing PBS 1X and 2% Fetal Calf Serum) and centrifuged at 300G for 3minutes at 4°C between fixation and proper incubations. Cells were analyzed in LSR Fortessa SORP (Becton-Dickinson) using BD FACSDiva™ software and subsequent data was analyzed using FlowJo™ software. Cell surface TNFα was assessed on the basis of mean fluorescence intensity (MFI), in arbitrary units.

**Crystal violet assay |** Cells were washed once with PBS and incubated with crystal violet solution (0.2% crystal violet assay, 2% ethanol and 97.8% $dH_2O$) filling the bottom of each well. After 30 minutes, cells were, carefully, washed with tap water by immersion in a large beaker. Approximately 1mL of 0.10% of acetic acid were added wells, before the reading of absorbance in Victor 3 1420-012 at 595nm.

**Statistical analysis |** Results are expressed as mean ± standard error of the mean (SEM). Statistical significance analysis was conducted by the two-way analysis of variance (ANOVA) with 95% confidence.

**Table 2.1: Reagents. Primary and secondary antibodies, transfection reagents, primers and TACE inhibitors used in the procedures described above.**

| Primary Antibodies | Brand, Reference | Host | Dilutions |
|---|---|---|---|
| **TNFα** | R&D System, #AF-410- | Goat | Western blot 1:500 |
| **Lamin B** | NA | Rabbit | Western blot 1:1000 |
| **NP** | AbCam®, #ab16048 | Rabbit | Immunofluorescence |
| **Rab11** | Invitrogen®, #715300 | Mouse | Immunofluorescence 1:1000 |
| **TNFα PE/Cy7 combined** | BioLegend® | Mouse | FACS 1:50 |
| **FLAG** | Sigma®, #F7425 | Rabbit | Western blot 1:2000 |
| **Secondary Antibodies** | **Brand, Reference** | **Host** | **Dilutions** |
| **Alexa Fluor® Anti-Rabbit 568** | Life technologies® #A-21068 | Goat | Immunofluorescence: 1:1000 |
| **Alexa Fluor® Anti-Mouse 647** | Life technologies® #A-21240 | Goat | Immunofluorescence: 1:1000 |
| **IRDye 800CW Donkey Anti-Mouse** | Li-Cor® #926-32212 | | Western blot: 1:10 000 |
| **IRDye 680RD Donkey Anti-Rabbit** | Li-Cor® #926-32214 | Donkey | Western blot 1:10 000 |

| Transfection Reagents | Brand, Reference | Concentrations |
|---|---|---|
| **Lipofectamine® LTX** | Life technologies®, #15338100 | Final concentration: 0.10% (v/v) |

| Primers | Sequence |
|---|---|
| **mTNFα-Forward** | CAGCCTCTTCTCATTCCTGC |
| **mTNFα-Reverse** | GGTCTGGGCCATAGAACTGA |
| **hTNFα-Forward** | TCAGCCTCTTCTCCTTCCTG |
| **hTNFα-Reverse** | GCCAGAGGGCTGATTAGAGA |
| **Actin-Forward** | CTACAATGAGCTGCGTGTGG |
| **Actin-Reverse** | AAGGAAGGCTGGAAGAGTGC |
| **GAPDH-Forward** | CTCTGCTCCTCCTGTTCGAC |
| **GAPDH-Reverse** | ACCAAATCCGTTGACTCCGAC |

| Plasmids | Description | Source |
|---|---|---|
| **pFLAG-TNFα** | pCR3 plasmid expressing TNFα with a N terminal FLAG tag | Colin Adrain – MT, IGC |
| **TACE inhibitors** | **Brand, Reference** | **Concentrations** |
| **MariMastat** | Calbiochem®, #44429-5MG | **5μM** |
| **BatiMastat (BB94)** | Calbiochem®, #196440-5MG | **10μM** |

# 3. Results

## Assay and tool development

## 3.1. Characterization of vRNP-Rab11 vesicles in HeLa cells infected by IAV

A prerequisite for the project was to establish cellular models to study the behaviour of Rab11 and the recycling endosome in response to influenza infection. We chose to begin with Hela cells, an adherent epithelial cell line. As shown in Figure 3.1, upon infection of Hela cells with influenza, the vRNA of Influenza A virus is replicated in the nucleus, exported to the cytoplasm as ribonucleoproteins (RNPs) and trafficked to the plasma membrane binding to Rab11 vesicles[121], the protein that regulates the slow host recycling pathway described in the introduction. Newly synthesised vRNPs that reach the cytoplasm, initially concentrate around the microtubule organizing centre (MTOC), but then become distributed throughout the cytoplasm, in puncta that enlarge during infection (Figure 3.1 A) and co-localise with Rab11, showing that vRNPs not only use the recycling pathway but also alter its structure and function. In agreement with this premise, it was shown that vRNP binding to Rab11-GTP, outcompetes that of Rab11-Family-interacting proteins, which are *bona fide* cognate binding partners of Rab11 in the healthy cell[125]. As a consequence, the normal flow of the recycling endosome becomes impaired as measured by the recycling of transferrin[125].

Analysis of the viral induced alteration in Rab11 vesicular morphology and cellular distribution was extended to several strains of virus and quantified in different cell types, including HeLa cells. Quantification was done by measuring the size distribution of Rab11 vesicular areas during a time course of IAV infection, assigning vesicles to three different categories: small (ranging 0 to 0.15 $\mu m^2$):, medium (0.15 to 0.30 $\mu m^2$) and large (>0.30 $\mu m^2$). As shown in Figure 3.1B, the number of vesicles of small size starts decreasing at 6 h p.i., coincident with the time at which vRNPs leave the nucleus giving rise to medium and large-sized vesicles. Cells impeded of releasing vRNPs from the cytoplasm or having a deficient Rab11, unable to bind to vesicles, fail to redistribute Rab11 during infection and this molecule does not co-localise with vRNPs and in these cells the virus replicated 100 times less[124]. In conclusion, this experiment indicated that, as expected, influenza infection perturbs the size and morphology of Rab11-containing recycling endosomes, indicating that the model is valid for the study of the recycling endosome.

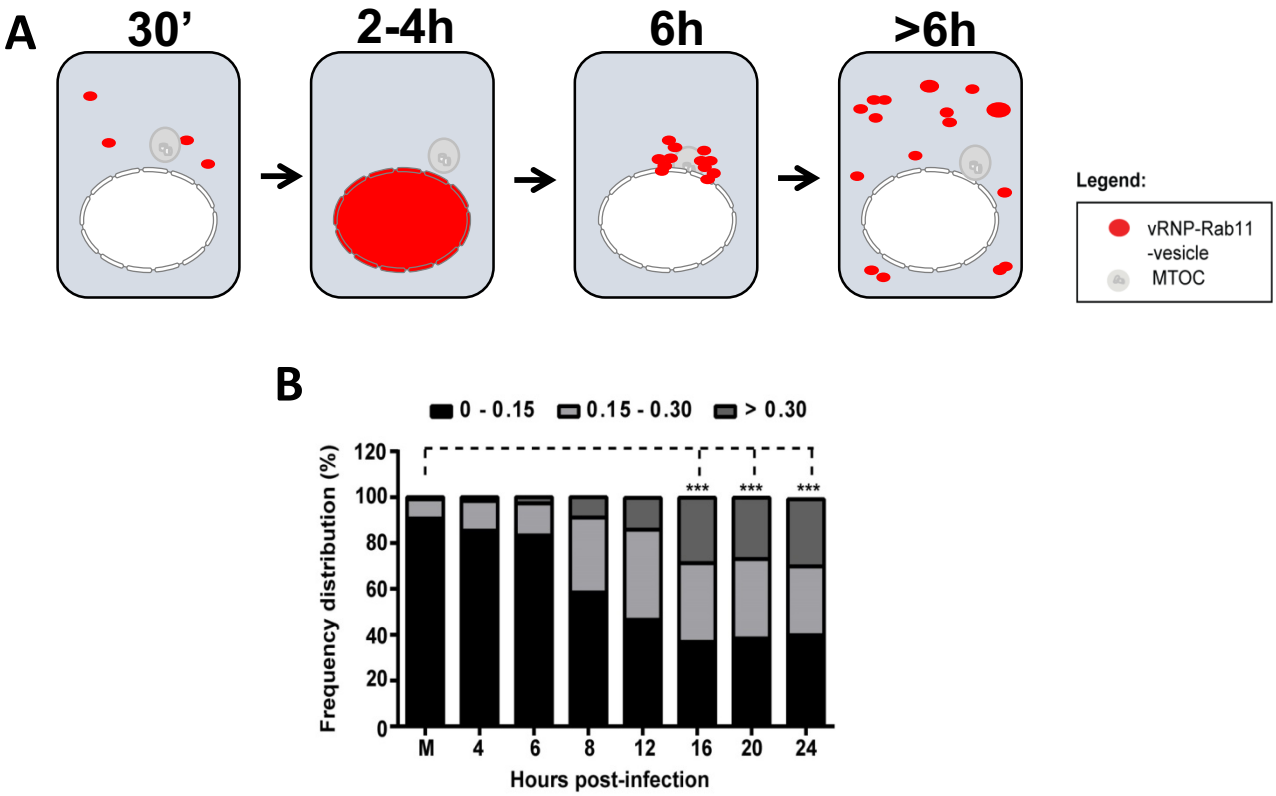


**Figure 3.1 | Time course of vRNPs localisation and Rab11 vesicles in HeLa infected cells.** A) Early in infection, vRNA accumulates in nucleoplasm. At later times, vRNPs accumulate near the MTOC and then bind to Rab11 to be transported to the periphery of the cell. B) The area of Rab11 (and NP) vesicles increases with time post-infection. The graph presents the frequency distribution of vesicles within the three size categories (small, medium and large). Illustration by MJ Amorim and graph from[125]

## 3.2. Transport of overexpressed TNFα in HeLa cells lines stably expressing Rab11 WT or Rab11 DN

As Hela cells are therefore a valid model for the study of Rab11, the next step was to obtain tools that would enable perturbing the Rab11 system. To do this, we obtained stable Hela cell lines expressing GFP-Rab11 WT and GFP-Rab11 DN. TNFα is not normally expressed in HeLa cells. However, the usage of Rab11 pathway is very well characterised in IAV infection in these cells, and it is well established that the recycling pathway changes in infection. In fact, it was shown that Rab11 pathway becomes impaired during IAV infection and therefore we decided as an initially strategy to assess if TNFα overexpressed in HeLa cells would, as shown for macrophages, use Rab11 pathway to reach the surface[23].

In order to test for a role of Rab11 in TNFα delivery to the surface, HeLa cells, HeLa GFP-Rab11 WT and HeLa GFP-Rab11 DN stable cell lines were transfected with a TNFα plasmid. The different cell lines contain a wild-type (WT) Rab11 expressed at either endogenous levels (HeLa), or overexpressed (HeLa GFP-Rab11 WT), and an inactivated Rab11 (HeLa GFP-Rab11 DN) where the effects of this molecule can be tested in TNFα secretion. Prior to assessing the effect of Rab11 or its mutants, to ensure that the experiments were properly controlled and that only the trafficking of TNF was being studied, I first assessed if the levels of TNF mRNA (3.2.1) and protein (3.2.2) were similar in all cell types.

### 3.2.1. TNFα mRNA levels in HeLa stable cell lines

mRNA levels of TNFα were quantified by RT-qPCR in the three cell lines, either untreated or treated with TACE inhibitor (iTACE). As mentioned in the introduction, TNFα needs to be cleaved by the protease TACE at the cell surface to be secreted. TACE inhibitor was used in this experiment for facilitating the analysis of protein expression for the following reasons. First, because iTACE blocks the ability of TACE to cleave TNF. It therefore increases the levels of TNFα in the cell and thus allows to better detect TNFα by western blot and; second as a means to test the antibody specificity, by detecting changes in the amount of the two forms of TNFα: the uncleaved[141] (of 26KDa, whose levels in the presence of iTACE would increase) and the cleaved form (of 17KDa, that in cells treated with iTACE would be absent). Although iTACE was used to assess protein rather than mRNA levels, there is the necessity to check if iTACE influences the levels of TNF transcription.

Results, presented in Figure 3.2, show that transfection was efficient and that the RT-qPCR was specific for TNFα. First, no mRNA levels were detected in non-transfected HeLa cells (mock samples). Second, upon transfection TNFα mRNA was detected at high levels. Importantly, the levels of mRNA of TNFα were similar between stable cell lines. Furthermore, no variations of mRNA levels were observed with the iTACE treatment. Having confirmed that the levels of TNF mRNA are largely unaffected by the expression of the Rab11 constructs, we next focussed on expression of the TNF protein itself.

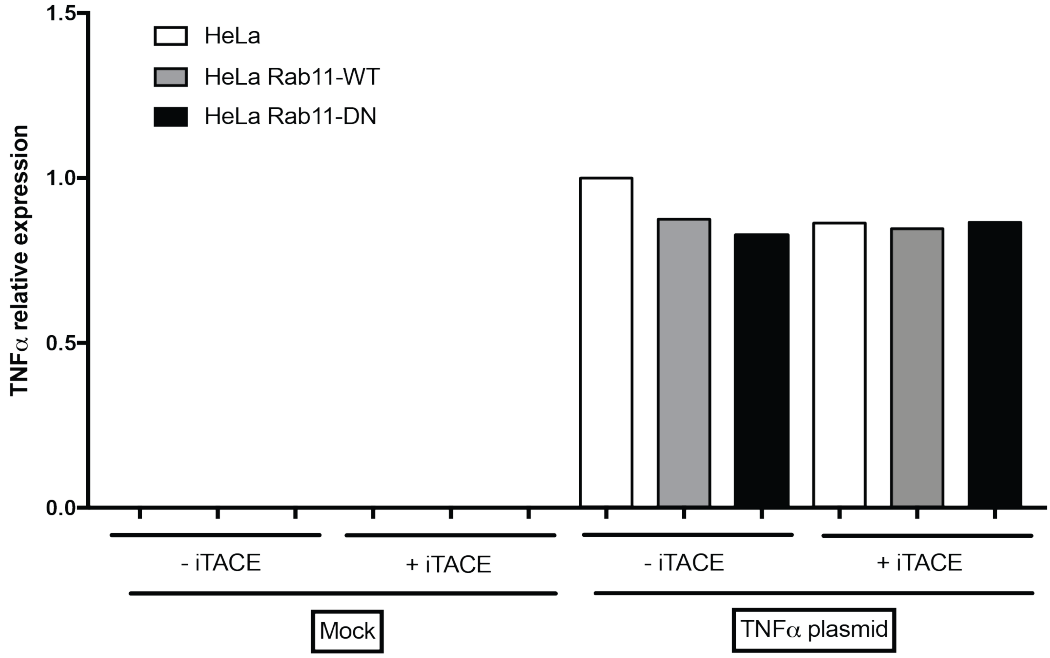


**Figure 3.2 | TNFα mRNA levels of cells treated with TACE inhibitor.** HeLa cells and HeLa stably expressing GFP-Rab11 WT and GFP-Rab11 DN cells were transfected with TNFα plasmid and treated with TACE inhibitor (iTACE). Cells were harvested and RNA was extracted from cells and reverse transcribed into a cDNA. Quantification of TNFα mRNA was evaluated by RT-qPCR and normalized relative to the mRNA of a housekeeping gene, GAPDH. No differences were verified between different conditions with and without treatment. The assay was performed once.

### 3.2.2 Characterization of the TNFα whole expression in HeLa stable cell lines.

Once we had confirmed the relative uniformity of mRNA levels of TNFα in HeLa stable cell lines, we evaluated the expression of TNFα by western blot. As above a sample was included with the iTACE treatment, and in addition we also included an extra sample treated with LPS. LPS is a glycolipid that constitutes the membrane of Gram-bacteria and when added to cells activates the release of pro-inflammatory responses in immune cells but also in epithelial cells[18]. As LPS will be systematically used to stimulate macrophages in future experiments, it was also included here as a control.

As shown in Figure 3.3 five bands could be detected: two bands of higher molecular weight ~26 KDa that could correspond to uncleaved or pro-TNFα, two bands at around ~17KDa that could correspond to the cleaved TNFα. In addition, one band in the middle of the gel is likely to be a non-specific background band that has a molecular weight that does not match either the pro- or cleaved TNFα molecular weight. Upon treatment with iTACE, the upper bands of the doublets appearing at 26KDa and 17KDa fluctuate. As expected, upon iTACE treatment, the pro-TNFα

levels increase and the cleaved form becomes absent, allowing to conclude that the upper bands of the doublets are indeed TNFα.

The levels between the different cell types (HeLa, HeLa Rab11 WT and HeLa Rab11 DN) of both cleaved and unprocessed TNFα are similar. This allows us to conclude that Rab11 does not impact on the translation of TNFα. It further indicates that Rab11 does not impact on the levels of the TNF transmembrane precursor, nor on the levels of the secreted species. In conclusion, this data does not support a role for Rab11 in the trafficking of TNF. We therefore decided to proceed to a more physiological setting for the study of the impact of Rab11 on TNF trafficking/secretion: macrophages, which are the primary synthesisers of this pro-inflammatory cytokine and hence a more physiological setting.

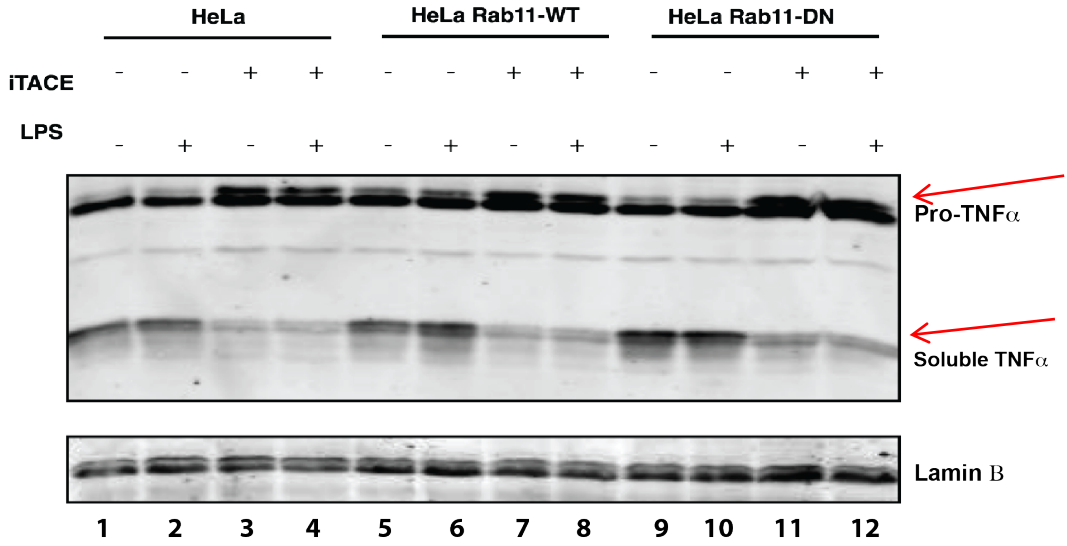


**Figure 3.3 | TNFα expression in HeLa cells treated with TACE inhibitor (iTACE).** HeLa and HeLa stably expressing GFP-Rab11 WT and GFP-Rab11 DN were stimulated with LPS during 2 hours and TACE inhibitor for 1 hour. Cells were harvested and proteins separated in a 17.5% acrylamide gel. Expression of TNFα was analyzed by western blotting on membranes stained for TNFα. Lamin B was used as a loading control. Pro-TNFα corresponds to the high molecular weight, inactivated TNFα and soluble TNFα correspond to TNFα cleaved by TACE. This figure is a representation of two independent experiments.

## 3.3. Characterization of Raw264.7 cells infected by IAV

To investigate the role of Rab11 in vRNP and in TNFα trafficking in macrophages, we used Raw264.7 cells with endogenous levels of Rab11, stably expressing GFP-Rab11 WT or GFP-Rab11 DN.

Initially, we had to understand if 1) macrophages were susceptible to IAV infection as recent reports suggest that raw cells are not permissive to infection[142]. In order to characterize the IAV infection in macrophages, the three raw cell lines were infected at a MOI of 3 with one of the following viruses: PR8 WT (henceforward PR8), PR8 ΔNS1 (henceforward ΔNS1) and X31.

We used these viruses for the following reasons. PR8 virus is the model virus for which the lab has many tools, including antibodies, primers, and probes. However, it is well-established that this virus is very efficient at impairing activation of innate immunity[143]. The most potent viral factor able to interfere with induction of innate immunity is the NS1 viral protein. Hence, we engineered a ΔNS1 mutant virus for achieving maximal levels of TNFα. This virus was made using a mutated version of segment 8 that lacked full-length NS1[144] (figure 3.4 B). Basically, a codon stop was added to the nucleotide 243 (amino acid 81). Thus, the virus expresses the first 81 amino acids of NS1 protein and totally express NS2 protein (as known as NEP) because NS2 has the first 30 nucleotides in common with NS1, then has an intron that NS1 does not possess and continues from nucleotide 529 to nucleotide 864.

X31 virus is a reassortant virus carrying HA and NA segments from 1968 Hong Kong influenza A virus but sharing the remaining segments from PR8 (Figure 3.4 C). This virus provokes a high immune response in infected cells.

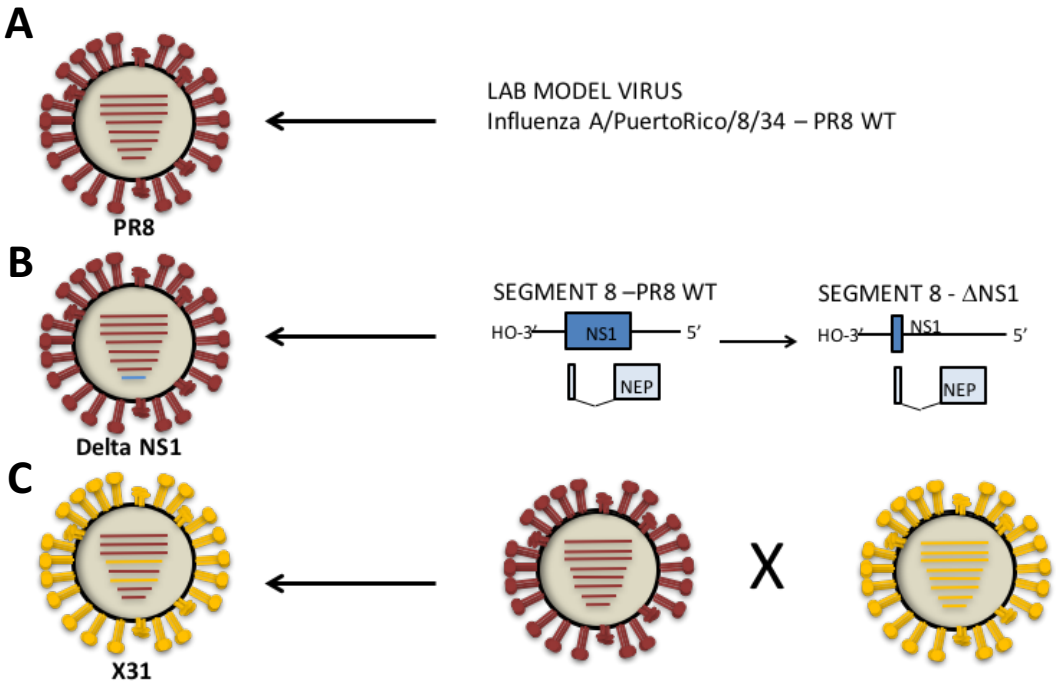


**Figure 3.4 | Characterization of PR8, ΔNS1 and X31 viruses. A)** PR8 is the wild-type lab model virus used. **B)** Schematic representation comparing segment 8 in PR8 WT and in PR8 ΔNS1 virus. ΔNS1 virus has a mutated version of segment 8 that lacked full-length NS1 **C)** Schematic representation of X31 virus. X31 is a recombinant virus that carries HA and NA segments from 1967 Hong Kong influenza A virus but shares the internal segments from PR8 wild-type. Illustration was a gift of MJAmorim.

### 3.3.1 IAV replicates in Raw264.7 cells

IAV infection in macrophages is not well characterised. A recent report for example showed that RAW macrophages are not permissive to PR8 infection[129].

In order to understand if IAV replicates in Raw264.7 cells, plaque assays were done. Stable cell lines were infected at a MOI of 3 with PR8, ΔNS1 or X31 virus for 16 hours. Supernatants were collected and processed as describe in chapter 2. Viral production was estimated by counting plaque forming units (PFU) per mL.

These experiments revealed that PR8 viral production was similar in all cell lines and indicated that PR8 replicates efficiently in these macrophages (Figure 3.5).This result does not corroborate the recent report by Marvin et al that showed that RAW macrophages are not permissive to PR8 infection[129].

ΔNS1 viral production is also similar between cell lines, but this virus presented a 10-fold reduction in viral production compared to PR8 (Figure 3.5). Regarding infection with X31, viral replication was impaired in all cell lines by a yet unclear reason.

Additionally, to further validate the previous results, a similar experiment with 8 hours infection was performed (in supplementary materials).

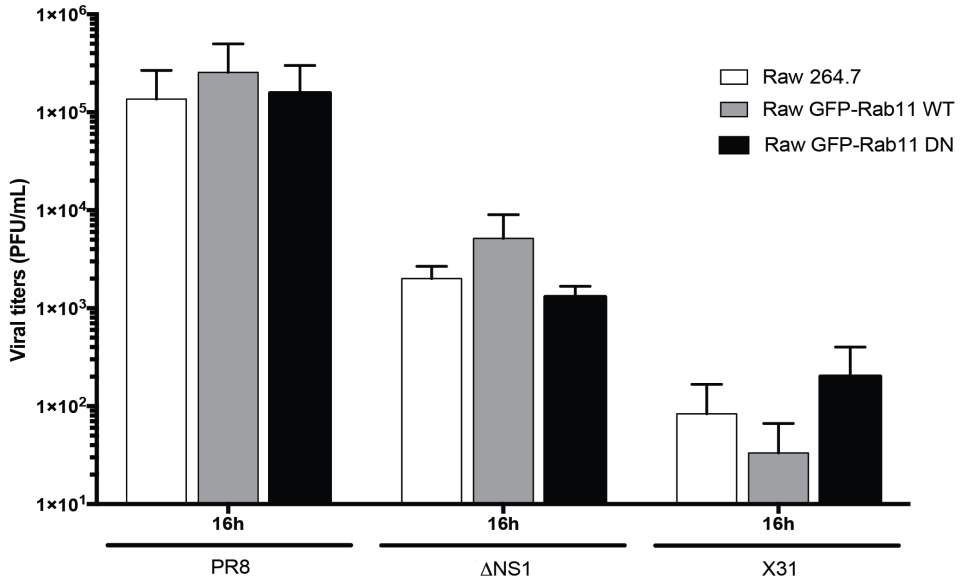


**Figure 3.5 | IAV replicates in Raw264.7 cells**. Raw264.7 and Raw264.7 cells stably expressing GFP-Rab11 WT and GFP-Rab11 DN were infected with PR8, ΔNS1 or X31 virus at a MOI of 3. At 16h p.i., supernatants were collected. MDCK cells were infected with the supernatants samples in serial dilution sets. 36 hours p.i. cells were fixed and stained using a 4% PFA - 0.2% toluidine blue solution. Plaque forming units were counted for each dilution and viral titers were estimated as PFU/mL. PR8 replicates efficiently in the cells. However, ΔNS1 and X31 viral production was deficient. The experiment was performed twice.

### 3.3.2 Characterization of NP-Rab11 vesicles in Raw264.7 cells infected by IAV

After confirming that macrophages are permissive to PR8 infection with minimal variations between cell lines for all viruses used, we decided to assess if vRNP associated with Rab11 by determining if 1) Rab11 and vRNPs co-localised and 2) if Rab11 distribution was altered during the course of infection. Thus, Raw264.7 and Raw264.7 stably expressing GFP-Rab11 WT or GFP-Rab11 DN were infected at a MOI of 3 with PR8, ΔNS1 or X31 virus and fixed at two time points. Cells were then stained for NP (a marker for vRNPs), Rab11 and counterstained with DAPI to mark the cell nucleus.

The three cell lines in mock infected cells behave as follows: GFP staining was detected in Raw GFP-Rab11 WT and Raw GFP-Rab11 DN, but not in Raw264.7 because these cells do not express a GFP form. In Raw264.7 cells, the Rab11 staining presents discrete dots throughout cytoplasm. In mock infected WT cells, GFP presents a punctuated staining pattern throughout cytoplasm as well as that of Rab11. While, in the case of the Rab11 DN cells, the distribution of Rab11-GFP is dispersed throughout the cytoplasm as is also observed when Rab11 is detected with Rab11 antibody, suggesting that Rab11 is not being recruited to vesicles.

I next examined the impact of IAV infection on Rab11 vesicle morphology.

**Raw264.7 cells infected with PR8 virus** show that as expected, at 8h p.i., NP is found distributed in discrete dots that co-localise with Rab11 in vesicles as measured by the Pearson's correlation coefficient (Figure 3.6D) that seems to increase with the course of the infection. Vesicular size can be visualised in Figure 3.6 A in images 5 to 6 and (for NP) and 8 to 9 (for Rab11). In images 11 and 12, the merge between both channels is depicted. Figure 3.6 B and C show the frequency distribution of the vesicles in terms of area. Both NP and Rab11 medium and large categories increase from mock to 16h p.i. indicating that as shown for HeLa cells the vesicular area increases with the course of infection.

**Raw GFP-Rab11 WT infected with PR8 virus** show at 8h p.i., NP is found distributed in discrete dots that co-localise with Rab11 in vesicles as measured by the Pearson's correlation coefficient. (Figure 3.6 D) that also seems to increase with the course of the infection. Vesicular size can be visualised in Figure 3.6 A in images 17 to 18 (for NP) and 20 to 21(for Rab11). In images 23 and 24, the merge between both channels is depicted. Figure 3.6 B and C show the frequency distribution of the vesicles in terms of area. Both NP and Rab11 present more vesicles in large category in 16h p.i. condition. Moreover, in this cell type, is possible to observe more vesicles in the large category which is due to the overexpressed Rab11 in this cell line, as observed in HeLa cells.

**Raw GFP-Rab11 DN infected with PR8** show total dispersion pattern for Rab11 and NP staining throughout the cytoplasm indicating that Rab11 and NP were not recruited to vesicles as seen for other cell types. These features can be found in images 25-27, 31-33 for Rab11, 29-30 for NP. The merge of both channels is shown in images 34-36 of figure 3.6 A.

In graphs 3.6 B and C of the Rab11 DN cells, vesicular size did not increase with infection, in agreement with what has been published in other cells. The Pearson's correlation coefficient is lower in these cells (Figure 3.6 D).

**All cell lines infected with ΔNS1 or X31 follow the same pattern as described for PR8:**

NP and Rab11 distribution in dots (vesicles) increases from mock to 16hpi, both visually and quantified in terms of areas (Figure 3.7 and 3.8 A-C). The Pearson's correlation coefficient is higher in GFP-Rab11 WT indicating an effective co-localisation between vRNPs and Rab11 (Figure 3.7 and 3.8 D).

Characterization of the vesicles in infected macrophages was similar to that described in the literature for other cell types including HeLa cells that we described in the beginning of this chapter. Thus, during IAV infection in macrophages, Rab11-GTP (and not GDP) is required to transport vRNPs to the cell surface. During the process, Rab11 distribution is altered, which is a proxy that indicates an impairment of the host cell recycling endosome.

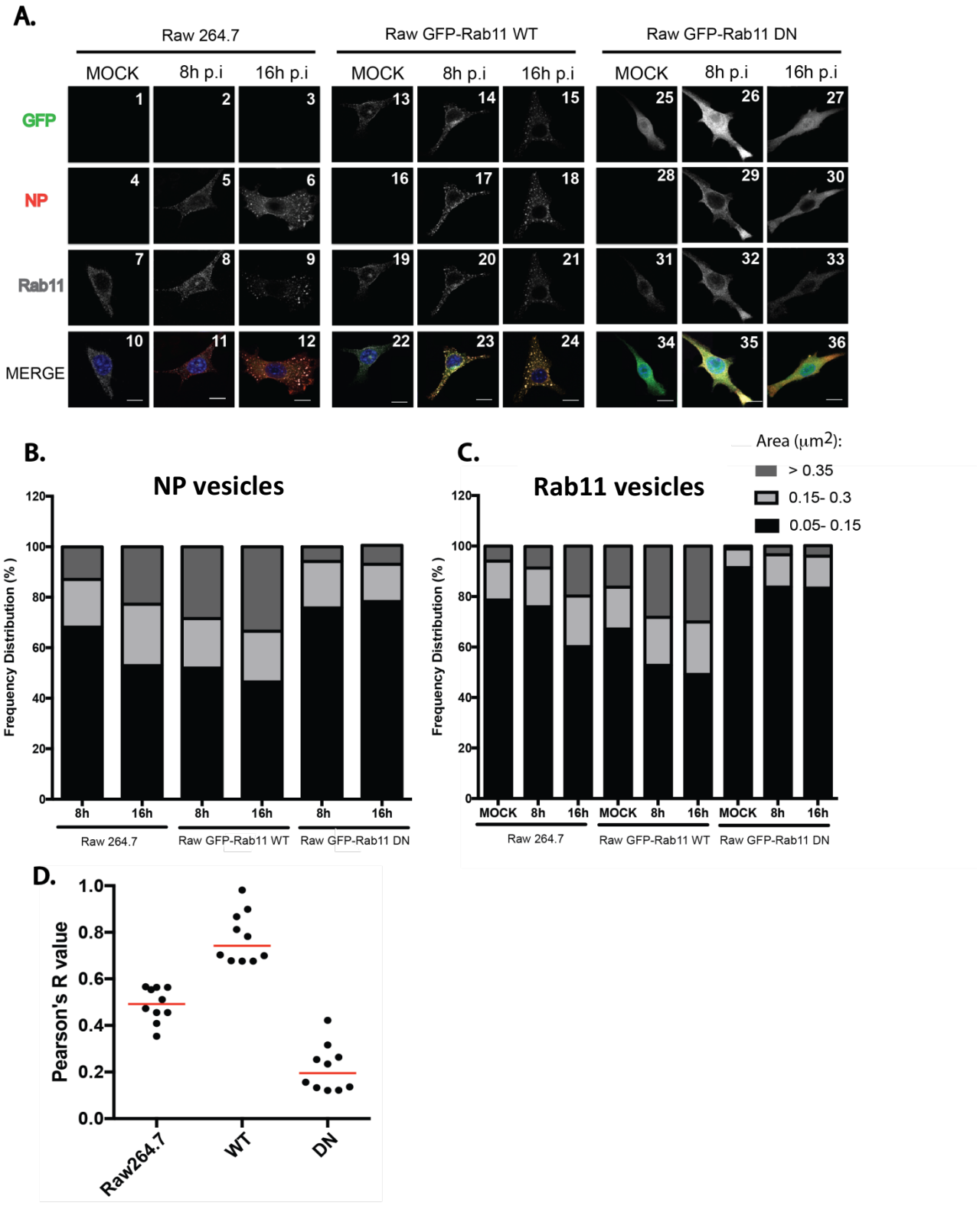


**Figure 3.6 | Characterization of PR8 infection in Raw264.7 stable cell lines expressing GFP-Rab11 WT and DN. A)** Stable cell lines were infected with PR8 virus at a MOI of 3. Upon fixation at the indicated time p.i., cells were immunostained against, NP and Rab11. Images were acquired by confocal microscopy (Leica SP5). Scale bars represent 10μm. Vesicular size was measured using a Fiji 'vesicle size' plugin, and the frequency distribution of three size categories (small, medium and large) was plotted in a graph taking into account NP **(B)** or Rab11 **(C).** Co-localisation of NP and Rab11 was measured through Person's correlation using Fiji plugin 'colocalization thresholds **(D)**. WT and DN cells correspond to Raw GFP-Rab11 WT and DN, respectively. Red dash represents the median of Person's R value. The assay was performed once and 15-30 cells were analysed.

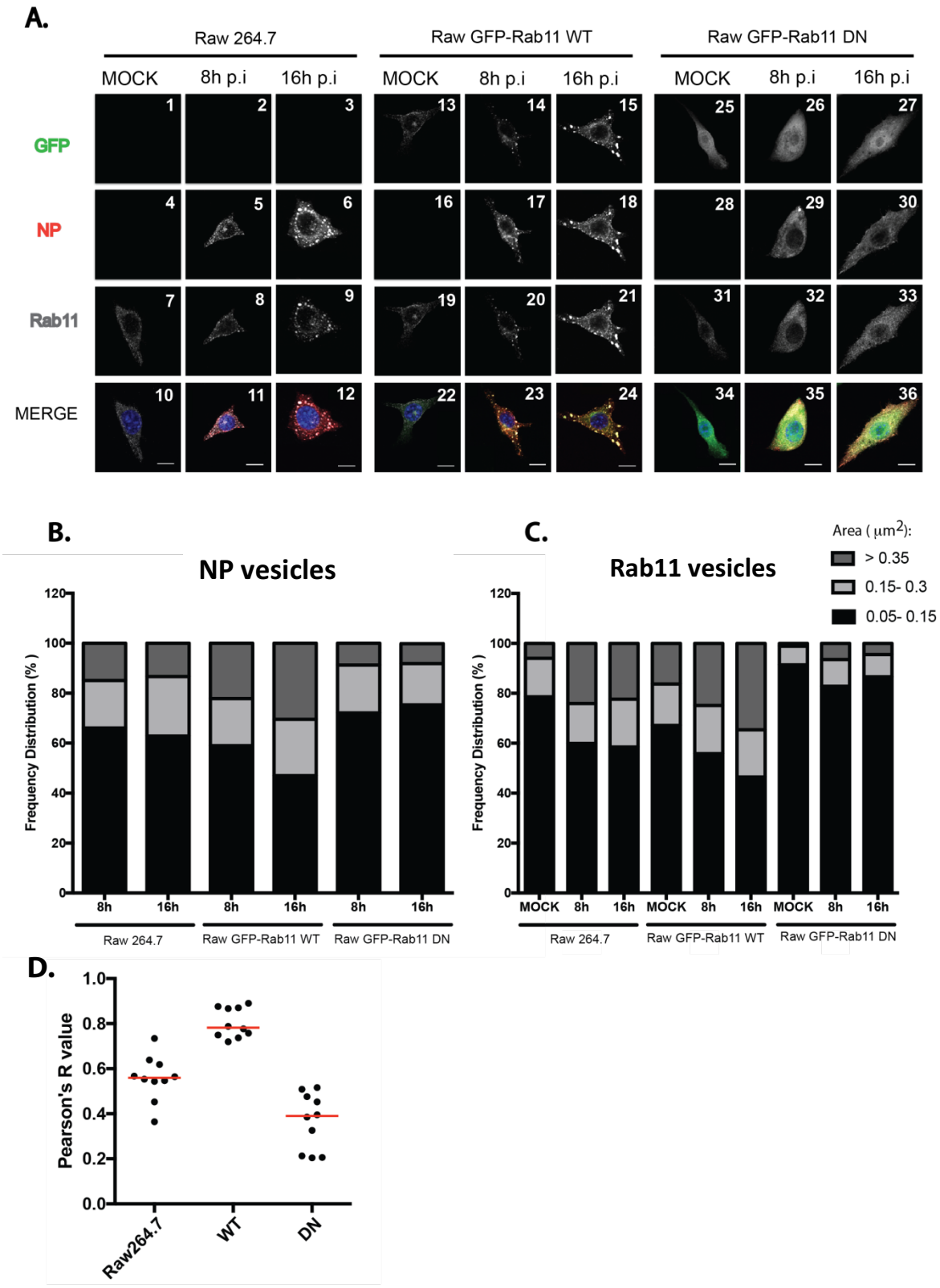


**Figure 3.7 | Characterization of ΔNS1 infection in Raw264.7 stable cell lines expressing GFP-Rab11 WT and DN. A)** Stable cell lines were infected with ΔNS1 virus at a MOI of 3. Upon fixation at the indicated time p.i., cells were immunostained against, NP and Rab11. Images were acquired by confocal microscopy (Leica SP5). Scale bars represent 10μm. Vesicular size was measured using a Fiji 'vesicle size' plugin, and the frequency distribution of three size categories (small, medium and large) was plotted in a graph taking into account NP **(B)** or Rab11 **(C).** Co-localisation of NP and Rab11 was measured through person's correlation **(D)** using Fiji plugin 'colocalization thresholds'. WT and DN cells correspond to Raw GFP-Rab11 WT and DN, respectively. Red dash represents the median of Person's R value. The assay was performed once and 15-30 cells were analysed.

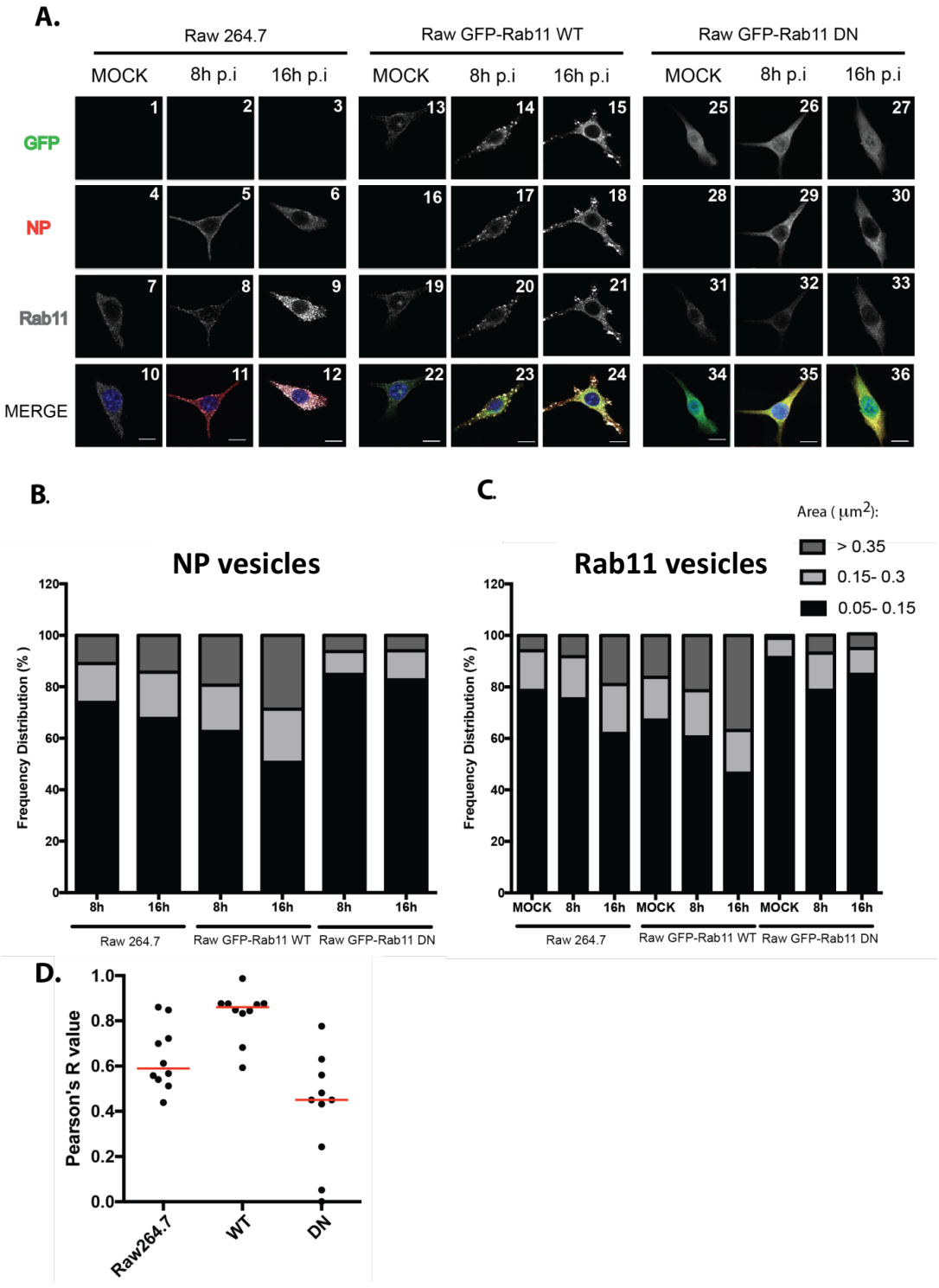


**Figure 3.8 | Characterization of X31 infection in Raw264.7 stable cell lines expressing GFP-Rab11 WT and DN. A)** Stable cell lines were infected with ΔNS1 virus at a MOI of 3. Upon fixation at the indicated time p.i., cells were immunostained against, NP and Rab11. Images were acquired by confocal microscopy (Leica SP5). Scale bars represent 10μm. Vesicular size was measured using a Fiji 'vesicle size' plugin, and the frequency distribution of three size categories (small, medium and large) was plotted in a graph taking into account NP **(B)** or Rab11 **(C).** Co-localisation of NP and Rab11 was measured through person's correlation **(D)** using Fiji plugin "colocalization thresholds'. WT and DN cells correspond to Raw GFP-Rab11 WT and DN, respectively. Red dash represents the median of Person's R value The assay was performed once and 15-30 cells were analysed.

# 3. Supplementary data

## IAV replicates in Raw264.7 cells

To assess the permissiveness of Raw cells to infection, we have not just done a titration at 16 h p.i. but also a time course. Stable cell lines were infected at MOI of 3 with PR8, ΔNS1 or X31 virus for 8 and 16 hours and virus titres were determined by plaque assays. Results show that for PR8 virus, the viral production increases 2 logs (100 fold) from 8 to 16 h p.i., while that of ΔNS1 does not increase and for X31, either a maintenance of even a reduction was observed, demonstrating the deficient viral production of these two viruses in Raw264.7 macrophages.

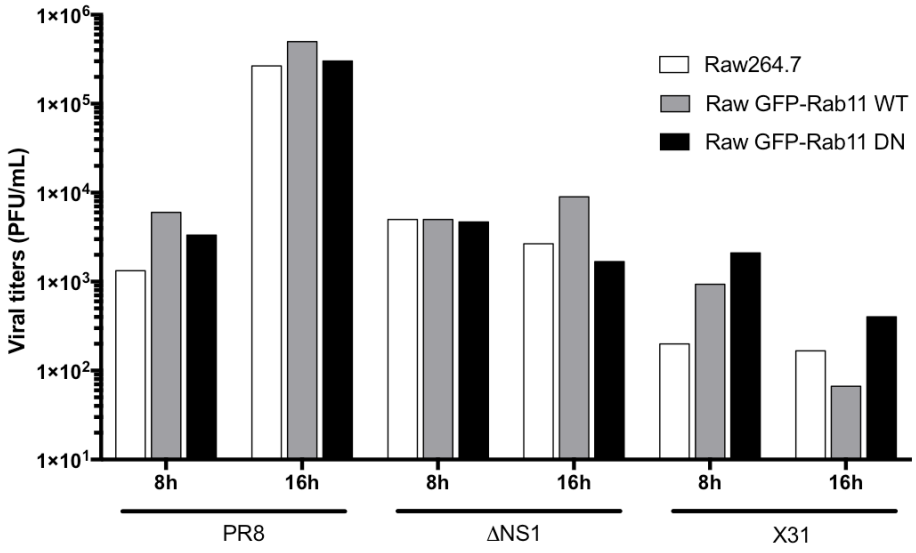


**Figure S3.1 | WT IAV replicates in Raw264.7 cells.** Raw264.7 and Raw264.7 cells stably expressing GFP-Rab11 WT and GFP-Rab11 DN were infected with PR8, ΔNS1 or X31 virus at a MOI of 3. At 8h and 16h p.i., supernatants were collected. MDCK cells were infected with these samples in serial dilution sets. 36 hours p.i. cells were fixed and stained using a 4% PFA - 0.2% toluidine blue solution. Plaque forming units were counted for each dilution and viral titers were estimated as PFU/mL. PR8 replicates efficiently in the cells. However, ΔNS1 and X31 viral production was deficient. The experiment was performed once.

# 4. Results

## 4.1. TNFα trafficking in Raw264.7 infected by IAV

### 4.1.1. TNFα mRNA levels in IAV infected cells

In order to test the effect of IAV infection in trafficking of TNFα, Raw264.7 cells and Raw264.7 cells stably expressing GFP-Rab11 WT and GFP-Rab11 DN were infected with PR8, ΔNS1 or X31 virus. After 14 hours, LPS was added to cells for 2 hours.

As previously mentioned, macrophages are activated by a variety of factors. In the lab, we can use LPS to stimulate macrophages and activate the immune responses recruited by membrane receptors that induce transcription and release of cytokines, including TNFα.

mRNA levels of TNFα were assessed by RT-qPCR in the three cell lines, both in infected and mock-infected.

Firstly, results presented in Figure 4.1 and table 4.1 (yellow cells), show that stimulation with LPS effectively activated transcription of TNFα, once higher levels of mRNA were detected for all conditions tested when LPS was present.

Concerning each cell line, no significant variations were observed between them, excluding ΔNS1 in which Raw GFP-Rab11 DN presented higher mRNA levels than Raw264.7, but this might be due to experimental error.

A statistical comparison between viruses in specific cell lines, showed that there are significant differences in TNFα induction. The orange cells in the table 4.1 illustrate these differences for each cell line. ΔNS1 and X31 viruses lead to a higher transcription of TNFα in all cell lines, when compared with PR8 virus. This behaviour was expected, because ΔNS1 and X31 provoke a high immune response in infected cell, as previously mentioned.

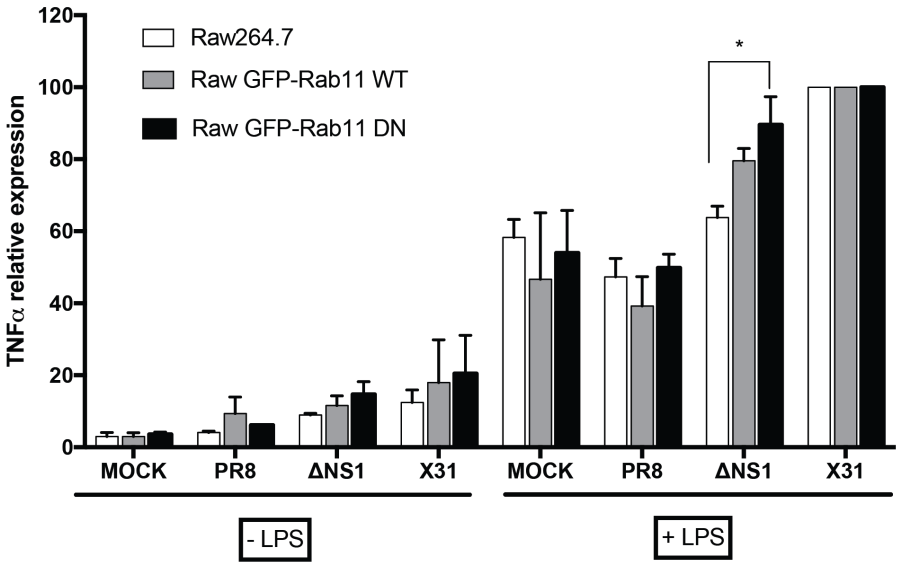


**Figure 4.1 | TNFα mRNA levels of infected cells.** Raw264.7 and Raw264.7 stably expressing GFP-Rab11 WT and GFP-Rab11 DN (represented in figure as WT and DN respectively) were infected with PR8, DNS1 and X31 virus at a MOI of 3. After 14h p.i, cells were stimulated with LPS and 16h p.i cells were harvested. RNA was extracted from cells and reverse transcribed into a cDNA. Quantification of TNFα was evaluated by RT-qPCR and normalized to actin values for each condition. All cells stimulated with LPS presented increased TNFα mRNA levels. All cells infected with DNS1 or X31 have higher TNFα mRNA levels. Two Way ANOVA test was performed, with confidence of 95%. (*) $P<0.05$. Figure is a representation of two independent experiments

**Table 4.1: Statistical analyses of TNFα mRNA levels in IAV infected cells. Two Way ANOVA test was performed, with confidence of 95%. (*) P<0.05.**

| | | Mock | | | PR8 | | | ΔNS1 | | | X31 | | |
|---|---|---|---|---|---|---|---|---|---|---|---|---|---|
| | | Raw + LPS | WT + LPS | DN + LPS | Raw + LPS | WT + LPS | DN + LPS | Raw + LPS | WT + LPS | DN + LPS | Raw + LPS | WT + LPS | DN + LPS |
| Mock | Raw | *** | * | ** | ** | | | *** | **** | **** | **** | **** | **** |
| | Raw + LPS | *** | * | ** | | | | *** | **** | **** | * | * | * |
| | WT | *** | * | ** | ** | ** | ** | *** | **** | **** | **** | **** | **** |
| | WT + LPS | *** | * | ** | * | ** | ** | *** | **** | * | *** | *** | *** |
| | DN | *** | * | ** | * | ** | ** | *** | **** | **** | ** | ** | ** |
| | DN + LPS | *** | * | ** | * | ** | ** | ** | *** | **** | **** | **** | **** |
| PR8 | Raw | *** | * | ** | | | | *** | **** | * | ** | ** | ** |
| | Raw + LPS | ** | * | ** | * | ** | ** | *** | **** | * | ** | ** | ** |
| | WT | ** | * | ** | * | * | * | *** | * | **** | *** | *** | *** |
| | WT + LPS | ** | * | ** | * | * | * | * | **** | **** | *** | *** | *** |
| | DN | ** | * | ** | * | * | * | *** | **** | **** | *** | *** | *** |
| | DN + LPS | ** | * | * | * | * | * | *** | **** | * | **** | **** | **** |
| ΔNS1 | Raw | ** | * | * | * | | | | | | **** | **** | **** |
| | Raw + LPS | ** | * | * | | | | | | * | **** | **** | **** |
| | WT | ** | * | * | * | | | | | | **** | **** | **** |
| | WT + LPS | ** | * | * | | | | | | | **** | **** | **** |
| | DN | * | * | * | | | | | | | **** | **** | **** |
| | DN + LPS | | | * | | | | | | | **** | **** | **** |
| X31 | Raw | ** | * | * | | | | | | | | | |
| | Raw + LPS | * | * | * | | | | | | | | | |
| | WT | * | * | * | | | | | | | | | |
| | WT + LPS | | | | | | | | | | | | |
| | DN | * | | | | | | | | | | | |
| | DN + LPS | | | | | | | | | | | | |

### 4.1.2. TNFα expression in IAV infected cells

Upon having established the similarity in the mRNA levels of TNFα upon IAV infection in the three Raw264.7 stable cell lines, we evaluated TNFα expression by western blot. Raw264.7 cells and Raw264.7 cells stably expressing GFP-Rab11 WT and GFP-Rab11 DN were infected with PR8, ΔNS1 or X31 virus and each sample was treated with LPS as above.

Figure 4.2 is a representative image of the results. For TNFα expression the western blot is distinct from the presented in Figure 3.3. Here, the upper band with the molecular weight of ~26kDa corresponds to uncleaved or pro-TNFα. The two bands which migrated around ~17kDa correspond to the cleaved, soluble TNFα.

Samples treated with LPS, as expected, have increased TNFα expression, when compared to untreated ones (for instance compare bands 1 and 2, Figure 4.2).
When we used PR8 to infect macrophages (in the presence or absence of LPS), we observed that levels of pro-TNFα are similar between the individual cell lines. In fact, the same result was verified in the other cells infected with ΔNS1 and X31 viruses. Whereas, when we observed the soluble TNFα is possible to detect several discrepancies among cell lines and viruses. Thus, we decided to evaluate TNFα expression in supernatants in order to evaluate the levels of released TNFα. Supernatants were collected and precipitated after 16 hpi. Again LPS treated samples have an increase in TNFα protein levels, no differences were observed between TNFα release amongst the different cell lines, for the virus used, suggesting that interference with Rab11 has no impact on TNF release.
Overall, we were unable to corroborate previous reports in which Rab11 was involved in TNFα trafficking in RAW macrophages. If Rab11 had a role in TNFα transport to the cell surface, lower levels of the soluble form would be observed as a consequence of a failure of TACE to cleave it, in GFP-Rab11 DN cells when compared with GFP-Rab11 WT. This was not the case.
Concerning the infection of the RAW cells with viruses, soluble TNFα levels from supernatants are decreased in samples infected with PR8 and ΔNS1 when compared with mock samples. This seems to indicate a disruption in TNFα trafficking provoked by IAV, once pro-TNFα levels are similar between viruses, while soluble TNFα levels are lower comparing to the mock samples.
Intriguingly, X31 infected-cells produce higher soluble TNFα levels when compared with PR8 and ΔNS1. The reason for that is not clear yet and requires further investigation.
However, we need to take in consideration that western blot is not a quantitative technique. To overcome this limitation, we tried to assess TNFα surface levels using flow cytometry (FACS). Nevertheless, we failed to obtain reliable results (see method troubleshooting in supplementary material of chapter 4 at the end of this chapter).

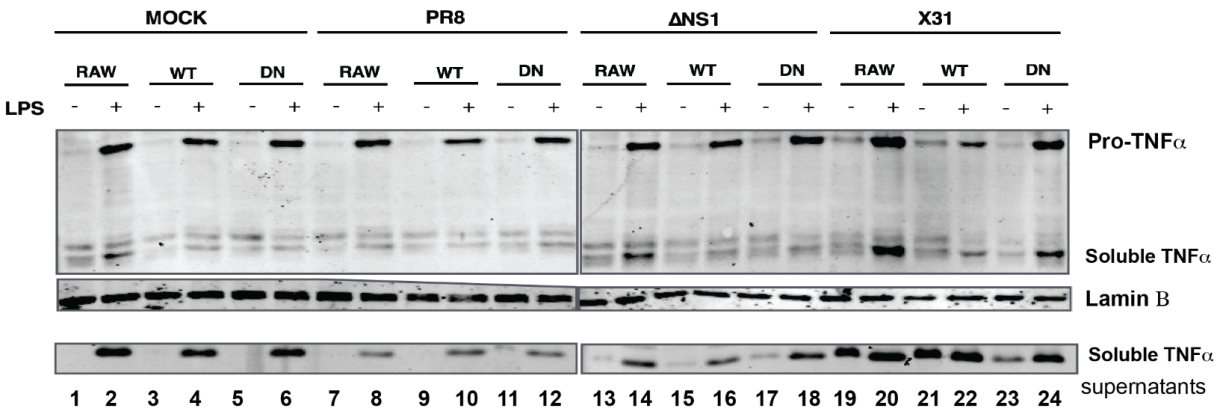


**Figure 4.2 | TNFα expression in infected cells.** Raw264.7 and Raw264.7 stably expressing GFP-Rab11 WT and GFP-Rab11 DN were infected with PR8, ΔNS1 or X31 virus at a MOI of 3. After 14h p.i, cells were stimulated with LPS for 2 hours. At 16h p.i., cells and respective supernatants are collected. Proteins in the supernatants were precipitated as described chapter 2. Cells and precipitated supernatants were diluted in Laemmli buffer. $5x10^4$ cells and supernatants were subject to electrophoresis on 17.5% acrylamide gel. Expression of TNFα was analyzed by western blotting on membranes stained for TNFα. Lamin B was used as a loading control. Pro-TNFα corresponds to inactivated TNFα and soluble TNFα corresponds to TNFα cleaved by TACE. This figure is a representation of three independent experiments.

### 4.1.3. Released levels of TNFα in IAV infected cells

Given the failure to confirm the western blot results by FACS, we decided to use a different strategy. We evaluated the released levels of TNFα by ELISA which is a highly quantitative, however expensive method. Raw264.7 cells and Raw264.7 cells stably expressing GFP-Rab11 WT and GFP-Rab11 DN were infected with PR8, ΔNS1 or X31 virus and each sample was treated with LPS as above. After 16h p.i., supernatants were collected and processed as described in materials and methods.

All conditions treated with LPS presented higher levels of TNFα (Figure 4.3). Between the different cell lines for each virus analysed no variations were observed, except and very likely due to experimental error for Raw264.7 cells in mock and PR8 infection in which more TNFα was observed. Due to time constraints, this experiment was performed only once, so these results require validation.

However, regardless such increase, these results indicate that Rab11 is not involved with the trafficking of TNFα, and corroborate our findings and not what was previously published[35]. After all, our prediction was that if Rab11 was important for TNFα transport in macrophages, the levels of TNFα in Raw GFP-Rab11 DN would show a tremendous decrease comparatively to Raw GFP-Rab11 WT, which was not the case.

Concerning the different viruses, it is possible to observe differences between them. Released TNFα levels in PR8 are similar to the mock, whereas, in ΔNS1 infected cells increased levels were observed. This result is consistent with what we see for transcription and translation. A similar observation was seen for X31 infected cells, being the virus that originates a higher release in TNFα for all cell lines when compared with the remaining viruses.

To control for the number of cells in these experiments, a crystal violet assay was performed. Figure 4.4 shows the optical density of each cell line demonstrating that we used an equivalent amount of each cell line per experiment.

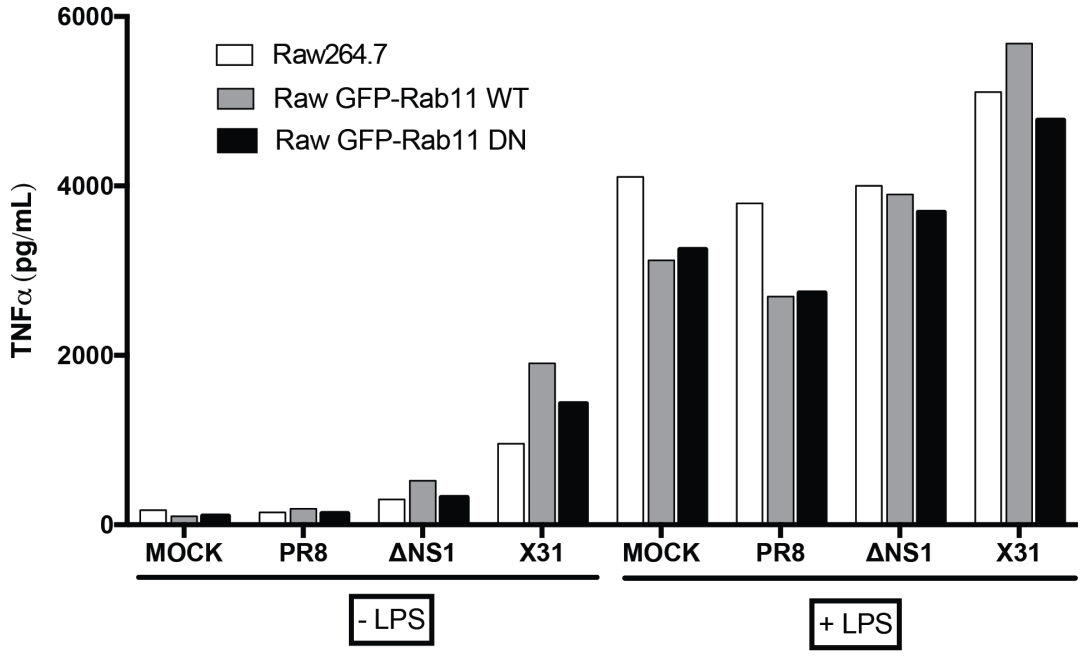


**Figure 4.3 | Levels of released TNFα from cells.** Raw264.7 and Raw264.7 stably expressing GFP-Rab11 WT and GFP-Rab11 DN were infected with PR8, DNS1 and X31 virus at a MOI of 3. After 14h p.i, cells were stimulated with LPS for 2 hours and supernatants were collected. Quantification of TNFα was evaluated by ELISA system (R&D system) as mentioned in chapter 2. Each condition was normalized to crystal violet values. All cells stimulated with LPS present higher levels of released TNFα. Assay was performed once.

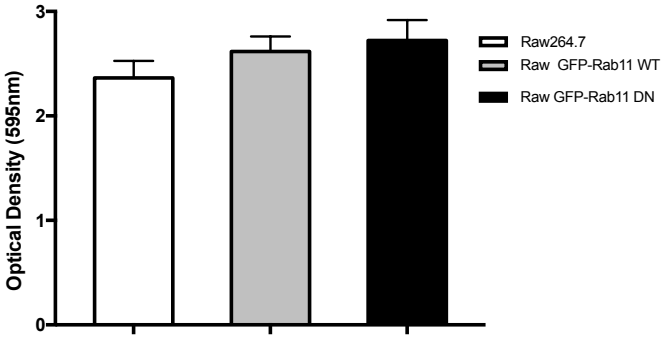


**Figure 4.4 | Crystal violet assay**. Graph shows the optical density of crystal violet stained cells. All cell lines presented similar values of optical density.

## 4.2 TNFα trafficking in cells inhibited for TACE

Our results suggest that in Raw264.7 cells, TNFα trafficking does not rely on Rab11-dependent trafficking pathways, which does not agree with previously published data[35]. We therefore decided to concentrate on validating the concept that TNFα trafficking in macrophages does not rely on Rab11. For this we did not use viruses, but rather TACE inhibitor (iTACE) in all Raw cell lines.

iTACE, as before, was used in this experiment to block TNFα in the plasma membrane facilitating the analysis of TNFα levels at the surface of the cells by increasing their levels in this region.

### 4.2.1 TNFα mRNA levels of cells treated with TACE inhibitor

mRNA levels of TNFα were quantified by RT-qPCR in the three cell lines treated or non-treated with iTACE and LPS.

Results, presented in Figure 4.5, show that all conditions treated with LPS presented higher mRNA levels of TNFα. Concerning the differences between cell lines, no significant variations were observed in cells treated or non-treated with iTACE which is in agreement with observed in the previous experiments.

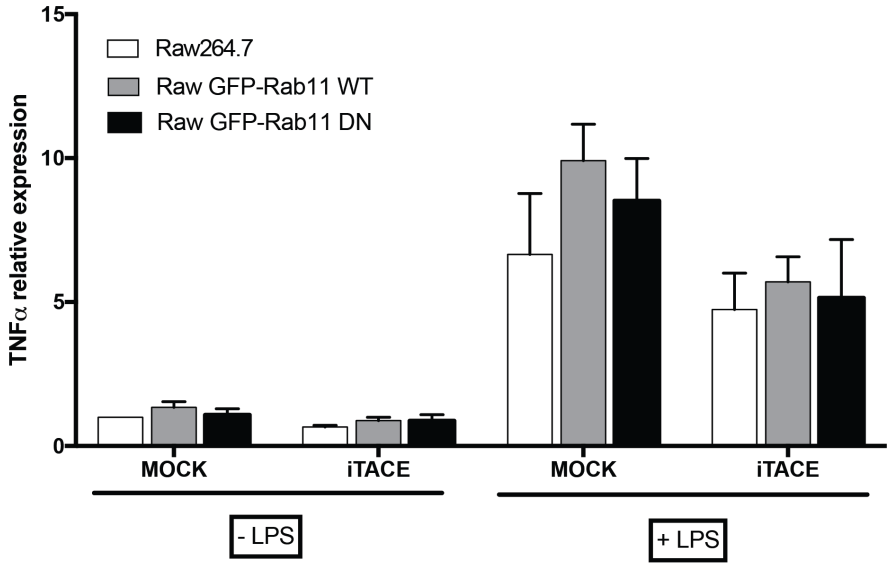


**Figure 4.5** | **TNFα mRNA levels of cells treated with TACE inhibitor (iTACE).** Raw264.7 and Raw264.7 stably expressing GFP-Rab11 WT and GFP-Rab11 DN cells were stimulated with LPS and treated with TACE inhibitor (iTACE). After 2 hours with LPS and 1 hour with iTACE, cells were harvested and mRNA was extracted from cells and reverse transcribed into a cDNA. Quantification of mRNA TNFα was evaluated by RT-qPCR and normalized to actin values for each condition. All cells stimulated with LPS presented increased TNFα mRNA levels. No differences were verified between different cell lines. Experiment is representative of two independent repeats.

## 4.2.2. TNFα surface levels in cells treated with TACE inhibitor

Confirmed the similarity of TNFα mRNA levels between the different cell lines upon iTACE treatment, we evaluated the TNFα levels at the surface of cells.

Figure 4.6 is a representative image of the results. LPS stimulation did not work in cells non-treated with iTACE. Probably, this was due to the antibody used. The process of cleavage and release of TNFα happens very fast and we believe that the antibody used is not adequate to detect the cleaved TNFα at the surface (see method troubleshooting in chapter 4 of supplementary material). When we treated cells with iTACE, the pro-TNFα is not cleaved, which permits the detection of TNFα at the surface. Despite the antibody limitation, if Rab11 had a role in TNFα trafficking, we would definitively observe a drastic decrease in TNFα levels at the surface in Raw GFP-Rab11 DN cells, which was not the case. These results corroborate our previous findings with the experiments using viruses, and validate the concept that TNFα trafficking in RAW macrophages does not rely on Rab11.

In these experiments, a crystal violet assay was also conducted to control the number of cells used in each treatment. (Figure 4.7).

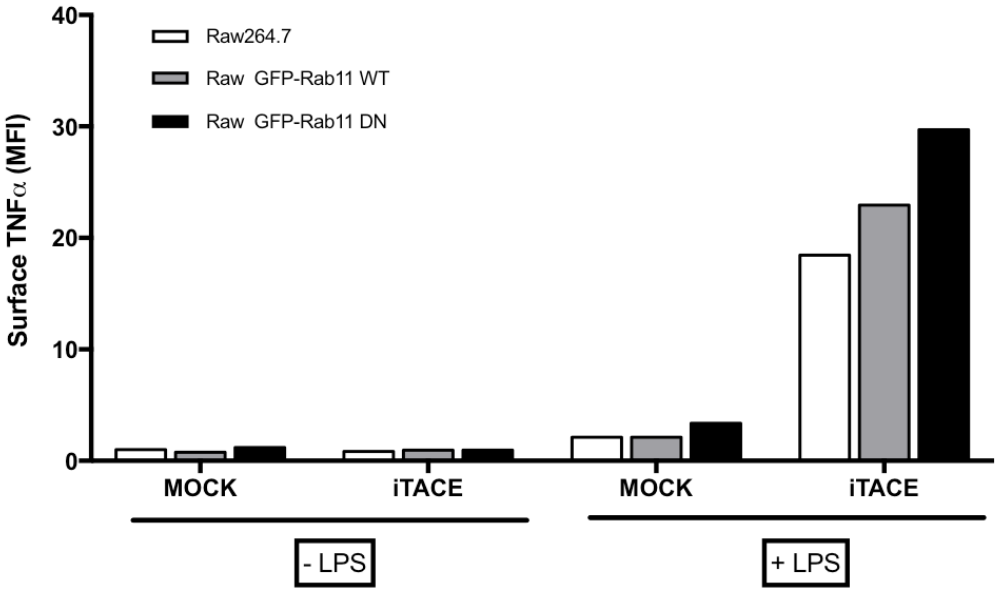


**Figure 4.6 | TNFα levels at the cell surface.** Raw264.7 cells and Raw264.7 stably expressing GFP-Rab11 WT and GFP-Rab11 DN cells were stimulated with LPS during 2 hours and treated with iTACE. Then, cells were harvested and fixed at in 4% PFA. Quantification of TNFα was evaluated by flow cytometry using LSR Fortessa machine. Experiment is representative of two independent repeats.

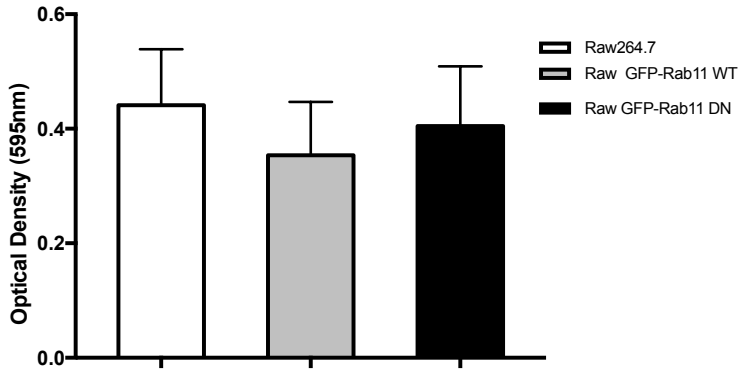


**Figure 4.7| Crystal violet assay**. Graph shows the optical density of crystal violet stained cells. All cell lines presented similar values of optical density.

# 4. Supplementary data

### Troubleshooting flow cytometry to analyse TNFα at the cell surface

We tried to perform FACS for the experiments described in the first part of chapter 4 (Figure S4.1). However, no differences were observed between samples stimulated with LPS suggesting a problem in the method used or with the antibody. For instance, TNFα cleavage at the cell surface could be a fast event and the antibody could be specific for the entire protein binding to an epitope only present in the pro-TNFα form.

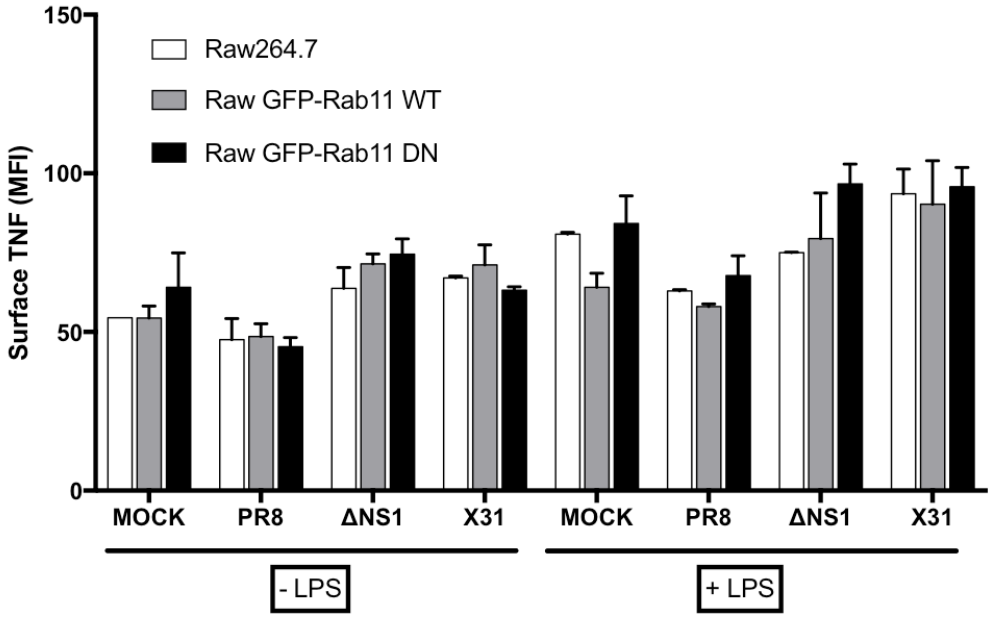


**Figure S4.1 | TNFα levels at the cell surface.** Raw264.7 and Raw264.7 stably expressing GFP-Rab11 WT and GFP-Rab11 DN were infected with PR8, ΔNS1 and X31 virus at a MOI of 3. After 14h p.i, cells were stimulated with LPS. Cells were harvested and fixed at 16h p.i in 4% PFA. Quantification of TNFα was evaluated by flow cytometry using LSR Fortessa machine. Cells stimulated with LPS did not present higher TNFα levels at surface due to experimental problems. Experiments are representative of two independent repeats.

Part of troubleshooting of the technique included using iTACE, to confirm if the antibody would just recognize an epitope on the whole TNFα. Figure S4.2 shows that in cells untreated with iTACE no differences in TNFα levels ate the cell surface were detected with LPS stimulation. Conversely, in cells incubated with iTACE and stimulated with LPS an increase of 30 times was observed in the levels of TNFα at. Taking together, these results, although preliminary permit to infer that the antibody recognizes the whole TNFα protein and that the cleavage of TNFα by TACE leads to the generation of a protein at the surface that the antibody we used can no longer see.

Therefore, we must analyse our data with cells infected with the different viruses using iTACE. However, due to time constraints, this was not possible.

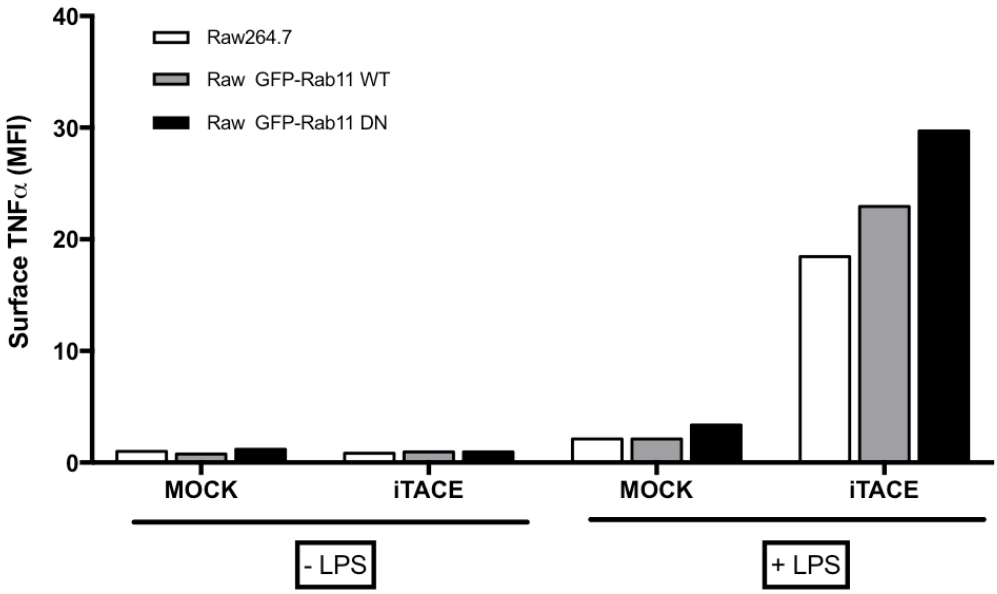


**Figure S4.2 | TNFα levels at the cell surface.** Raw264.7 cells and Raw264.7 stably expressing GFP-Rab11 WT and GFP-Rab11 DN cells were stimulated with LPS during 2 hours and treated with iTACE. Then, cells were harvested and fixed at in 4% PFA. Quantification of TNFα was evaluated by flow cytometry using LSR Fortessa machine. Experiment is representative of two independent repeats.

# 5. Discussion

TNFα is an important cytokine that regulates several mechanisms inside the body such as immune responses, haematopoiesis and tumorigenesis[2]. It also plays a role in specific diseases such as rheumatoid arthritis and diabetes[3].
Macrophages are one of the most prominent synthesizers of TNFα. In the presence of pathogens as viruses, macrophages release higher amounts of TNFα in order to recruit other cells of the immune system, preventing the propagation of the infection[57].

IAV is a critical human pathogen that provokes frequent epidemics worldwide[70]. Recent findings revealed that IAV uses the recycling endosomes for trafficking of the newly-synthesized viral genomes. The major regulator of this compartment, Rab11, is known to bind progeny vRNPs, upon nuclear export[125]. During infection the virus impairs the recycling endosome pathway[125]. TNFα has also been reported to use the recycling endosome and Rab11 to reach the cell surface in macrophages[35]. This project therefore had the goal to understand if the viral usage of the recycling endosome in infected macrophages could lead to a reduction in TNFα release and hence a decrease in the clearance of the virus.

This project focussed on the role of the Rab11 in trafficking of TNF and the ability of influenza to interfere with TNF trafficking and hence signalling by interference with Rab11 vesicles. We used as a preliminary system HeLa cells because these cells are well known for using Rab11 pathways upon IAV infection.
We used cell lines containing a WT Rab11 expressed at either endogenous levels (HeLa) or overexpressed (HeLa GFP-Rab11 WT) and an inactivated form of Rab11 (HeLa GFP-Rab11 DN). No variations in TNFα expression were detected in these cells, which indicates that the system could be used to address if HeLa cells used the recycling endosome to trafficking TNFα to the surface. However, TNF secretion was the same in all the cell lines, suggesting that Rab11 did not mediate trafficking of exogenously supplied TNFα in HeLa cells (Figure 3.3). For this reason, we decided to proceed with the evaluation of TNFα trafficking in macrophages, the cells used in the published data[35].

We next used, Raw264.7 cells and Raw264.7 stably expressing either GFP-Rab11 WT and DN were used to study the TNFα trafficking as well as the participation of the IAV in this process.
Initial experiments showed that IAV infected these macrophages (Figure 3.5). All cell lines presented similar viral production in each viruses used. PR8 virus replicated efficiently in these macrophages (Figure 3.5). These results did not corroborate the recent published data that show that Raw264.7 cells were not permissive to PR8 infection[129].

Concerning the ΔNS1 virus, a substantial reduction of viral production was observed. In fact, macrophages are more prepared to defend against ΔNS1 viruses, once this virus cannot efficiently prevent the activation of innate immune responses which could lead to a reduction in the viral production. In X31, viral replication was disrupted in all cell lines by a yet unclear reasons. By immunofluorescence (Figure 3.8), we observed that the virus is able to enter the cell, replicate, and vRNPs were found to leave the nucleus. We however, have not done a thorough quantification of the viral replication, nor have we evaluated all the steps in the viral lifecycle to be able to pinpoint at which stage the virus is being inhibited.

In addition, we characterized and quantified the NP-Rab11 vesicles in Raw264.7 cells infected by IAV in order to see if the virus used the recycling endosome to transport the vRNPs in this system. The results reproduced what had been published for HeLa cells. In Raw GFP-Rab11 WT cells and for all viruses, NP was found distributed in discrete dots that co-localised with Rab11, and the vesicular area increased with the course of the infection (Figure 3.6-3.8). On the other hand, Raw GFP-Rab11 DN cells showed a lack of co-localisation of Rab11 and NP and a dispersed staining throughout cytoplasm as expected and observed for HeLa cells. This results validated our system and allowed us to proceed with the evaluation of TNFα trafficking in infected and mock-infected cells.

Once confirmed the similarity in the mRNA levels of TNFα upon IAV infection in the three Raw264.7 cell lines we used, we evaluated the levels of TNFα expression in these cells.
Taken all together, the results showed no differences in the TNFα expression between the different cell lines which indicates that Rab11 is not involved in the transcription of TNFα mRNA (Figure 4.1). We confirmed that the levels of protein being expressed were also similar in the three cell lines. We assessed trafficking by two different manners, we examined the levels of TNF released (by the non-quantitative method western blot and by ELISA (Figure 4.2 and 4.3)), and both methods showed that Rab11 was not involved in TNFα trafficking and release. Our prediction was that if Rab11 was important for TNFα transport, the levels of TNFα released in Raw GFP-Rab11 DN would show a remarkable decrease when compared with that released from Raw GFP-Rab11 WT and Raw264.7 cells.

Concerning the different viruses used (PR8, ΔNS1 and X31), interesting differences were observed between them. PR8 virus presented, as expected, similar levels of TNFα comparatively with mock. This virus is more aggressive than ΔNS1 or X31 and does not permit an increase in the released TNFα levels due its high ability in disrupt the innate immune responses from the host.
Whereas, ΔNS1 infected cells release higher levels of TNFα The most interesting result was the one obtained with X31, once this virus originated higher mRNA levels of TNFα as well as higher released TNFα levels when compared to either PR8 and ΔNS1 viruses. X31 provokes a high immune response in infected cells similar to ΔNS1 and there is no apparent reason for the discrepancy between ΔNS1

and X31. At present we do not understand why X31 leads to this high levels of TNFα release, as X31 contains all the same segments to that of ΔNS1, except segments that codify for NA and HA. How these proteins affect innate immunity has not been reported and requires further investigation. Despite, the discrepancies between the different virus used, we did not observe differences between cell lines for each virus. These results indicate that IAV, as expected, modulates the TNFα trafficking in terms of suppression of innate immune responses from the cell which provokes higher or lower TNFα expression. However, the similarity between cell lines, in particular between Raw GFP-Rab11 WT and DN indicates that even if the virus impairs Rab11 pathway while transporting vRNPs to the surface, the same is not occurring for TNFα.

Given the results obtained, we decided to focus in validating that TNFα trafficking in macrophages does not rely on Rab11. Thus, we decided to stop using the virus and use TACE inhibitor instead. iTACE permitted to block the cleavage of TNFα from the plasma membrane, facilitating the measurement of TNFα levels at the surface of the cells.

The TNFα levels at the surface were analysed by FACS. We observed that there was no decrease in TNFα levels in Raw GFP-Rab11 DN cells when compared to Raw GFP-Rab11 WT (Figure 4.6). These results corroborate our previous results and validate our results using viruses showing the lack of involvement of Rab11 pathway in trafficking TNFα to the cell surface in Raw264.7 macrophages. Taking all these results, there are obvious incongruences between our data and published data[35].

Thus, the results obtained in this project raise the question: What are the differences between our system and the published system?
In this project we used macrophages stably expressing a WT Rab11 in which Rab11 can fluctuate between an active and an inactive form as well as a Rab11 form is permanently inactivated. Whereas, Jennifer Stow *et al* in[35] used macrophages transfected with a CA Rab11 that is permanently activated. Whether the DN-Rab11 stable cell lines acquire other strategies to transport TNFα to the surface requires investigation. Thus, we need to transfect Raw264.6 cells with a CA and a DN Rab11 and check at the surface the levels of TNFα to compare our data with published data.

In conclusions, our data suggests that TNFα does not rely on Rab11 to be transported to the surface on Raw264.7 cells.

# 6. Future perspectives

This project was designed to evaluate 1) IAV replication in macrophages and requirement of the recycling endosome to transport vRNPs, and 2) the role of Rab11 in TNFα transport in macrophages as well as 3) alterations in TNFα secretion upon IAV infection.

Concerning IAV replication in macrophages, our data suggest that there is production of PR8 in macrophages which did not corroborate the recent publish data[7]. One interesting aspect that came out of this project is to understand the contribution of NA and HA to TNFα release in infected cells because X31 virus presented higher levels of TNFα released comparatively with PR8 and the only differences between this two virus are the segment 4 (HA) and the segment 6 (NA).

The second aim of the project was to characterize the NP-Rab11 vesicles in Raw264.7 macrophages infected by IAV in order to comprehend if in these cells, IAV also use recycling endosome and Rab11 to transport vRNPs. Our data showed a similar behaviour of both cell types. To consolidate these data, we should repeat the experiment at least twice to obtain the statistical analysis and perform biochemical assays including pull down experiments.

Regarding the role of Rab11 in TNFα transport in macrophages, our study showed that there is no correlation between Rab11 and TNFα trafficking in the Raw264.7 cells.

However, we need to repeat the FACS data with transfected CA/DN Rab11 in macrophages and this manner we will be able to compare directly our data with the results from Jennifer Stow *et al*[35].
To dissect the secretory traffic of TNFα in macrophages, it would be interesting to study kinetically the trafficking of TNF using the RUSH (retention using selective hooks) system[145]. This system is a two-state assay exploiting the reversible interaction of a hook protein fused to streptavidin and stably anchored in the donor compartment (e.g. the endoplasmic reticulum, ER) with a reporter protein of interest. Upon adding biotin, the reporter is released from its ER hook, allowing to the assess by live-cell imaging and the kinetics of trafficking and trafficking route taken by the TNFα reporter from the ER to the plasma membrane.

Besides the immortalized cell line of macrophages (Raw264.7) used in this study, it would be interesting to isolate primary monocytes from mice and apply the same experimental setup to these cells. These cells are physiologically more relevant. The recycling endosome has been implicated in the secretion and display of other centrepieces in host immunity, in a cell dependent manner[35-146]. In macrophages and NK cells, the recycling endosome was implicated in the secretion of TNFα[35], IL10[30], IFN[59] and in phagocytosis[147]; and in epithelial cells in MHC-I presentation[146]. Thus, other parts

of the project could include the analyses of these other players in infection.

# 7. References

1. Bruns P. Die heilwirkung des erysipels auf geschwulste. *Beitr Klin Chir*. 1887;3(3):443-466.
2. Chan RWY, Leung CYH, Nicholls JM, Peiris JSM, Chan MCW. Proinflammatory Cytokine Response and Viral Replication in Mouse Bone Marrow Derived Macrophages Infected with Influenza H1N1 and H5N1 Viruses. *PLoS One*. 2012;7(11). doi:10.1371/journal.pone.0051057.
3. Clark IA. How TNF was recognized as a key mechanism of disease. *Cytokine Growth Factor Rev*. 2007;18(3-4):335-343. doi:10.1016/j.cytogfr.2007.04.002.
4. Kornbluth RS, Edgington TS. Tumor necrosis factor production by human monocytes is a regulated event: induction of TNF-alpha-mediated cellular cytotoxicity by endotoxin. *J Immunol*. 1986;137(8):2585-2591. http://www.jimmunol.org/content/137/8/2585.abstract.
5. Cheung CY, Poon LLM, Lau AS, et al. Induction of proinflammatory cytokines in human macrophages by influenza A (H5N1) viruses: A mechanism for the unusual severity of human disease? *Lancet*. 2002;360(9348):1831-1837. doi:10.1016/S0140-6736(02)11772-7.
6. Locksley RM, Killeen N, Lenardo MJ. The TNF and TNF receptor superfamilies: integrating mammalian biology. *Cell*. 2001;104(4):487-501.
7. Weiss T, Grell M, Siemienski K, et al. TNFR80-dependent enhancement of TNFR60-induced cell death is mediated by TNFR-associated factor 2 and is specific for TNFR60. *J Immunol*. 1998;161(6):3136-3142.
8. Mukhopadhyay A, Suttles J, Stout RD, Aggarwal BB. Genetic deletion of the tumor necrosis factor receptor p60 or p80 abrogates ligand-mediated activation of nuclear factor-κB and of mitogen-activated protein kinases in macrophages. *J Biol Chem*. 2001;276(34):31906-31912.
9. Feinberg B, Kurzrock R, Talpaz M, Blick M, Saks S, Gutterman JU. A phase I trial of intravenously-administered recombinant tumor necrosis factor-alpha in cancer patients. *J Clin Oncol*. 1988;6(8):1328-1334.
10. Gardam MA, Keystone EC, Menzies R, et al. Anti-tumour necrosis factor agents and tuberculosis risk: mechanisms of action and clinical management. *Lancet Infect Dis*. 2003;3(3):148-155.
11. Manderson AP, Kay JG, Hammond LA, Brown DL, Stow JL. Subcompartments of the macrophage recycling endosome direct the differential secretion of IL-6 and TNF?? *J Cell Biol*. 2007;178(1):57-69. doi:10.1083/jcb.200612131.
12. Nigrovic PA, Lee DM. Mast cells in inflammatory arthritis. *Arthritis Res Ther*. 2005;7(1):1-11. doi:10.1186/ar1446.
13. Kagoya Y, Yoshimi A, Kataoka K, et al. Positive feedback between NF-κB and TNF-α promotes leukemia-initiating cell capacity. *J Clin Invest*. 2014;124(2):528-542.
14. Dawicki W, Marshall JS. New and emerging roles for mast cells in host defence. *Curr Opin Immunol*. 2007;19(1):31-38.
15. Brinkmann MM, Spooner E, Hoebe K, Beutler B, Ploegh HL, Kim YM. The interaction between the ER membrane protein UNC93B and TLR3, 7, and 9 is crucial for TLR signaling. *J Cell Biol*. 2007;177(2):265-275. doi:10.1083/jcb.200612056.
16. Black Et Al 1997.Pdf.
17. Xaus J, Comalada M, Valledor AF, et al. LPS induces apoptosis in macrophages mostly through the autocrine production of TNF-α. *Blood*. 2000;95(12):3823-3831.
18. K È, Eissner G, Differences PM, Activation L. Differences in LPS-Induced Activation of Bronchial Epithelial Cells ( BEAS-2B ) and Type II-Like Pneumocytes ( A-549 ). 2002:294-302.
19. Peschon JJ, Torrance DS, Stocking KL, et al. and p75 in Several Models of Inflammation. *J Immunol*. 1998;160:943-952.
20. Horiuchi T, Mitoma H, Harashima S, Tsukamoto H, Shimoda T. Transmembrane TNF-α: structure, function and interaction with anti-TNF agents. *Rheumatology (Oxford)*. 2010;49(7):1215-1228. doi:10.1093/rheumatology/keq031.
21. Shearer WT, Reuben JM, Mullington JM, et al. Soluble TNF-α receptor 1 and IL-6 plasma

levels in humans subjected to the sleep deprivation model of spaceflight. *J Allergy Clin Immunol*. 2001;107(1):165-170.
22. Bandman O, Lal P, Guegler KJ, Shah P, Corley NC. Vesicle trafficking proteins. May 2011.
23. Murray RZ, Stow JL. Cytokine secretion in macrophages: SNAREs, Rabs, and membrane trafficking. 2014.
24. Rosenfeld MG, Marcantonio EE, Hakimi J, et al. and Processing of in the Endoplasmic Reticulum. *J Cell Biol*. 1984;99:1076-1082.
25. Cheung PFY, Wong CK, Lam CWK. Molecular mechanisms of cytokine and chemokine release from eosinophils activated by IL-17A, IL-17F, and IL-23: implication for Th17 lymphocytes-mediated allergic inflammation. *J Immunol*. 2008;180(8):5625-5635.
26. Mori R, Ikematsu K, Kitaguchi T, et al. Release of TNF-α from macrophages is mediated by small GTPase Rab37. *Eur J Immunol*. 2011;41(11):3230-3239.
27. Goud B, Gleeson PA. TGN golgins, Rabs and cytoskeleton: regulating the Golgi trafficking highways. *Trends Cell Biol*. 2010;20(6):329-336.
28. Wu M, Lu L, Hong W, Song H. Structural basis for recruitment of GRIP domain golgin-245 by small GTPase Arl1. *Nat Struct Mol Biol*. 2004;11(1):86-94.
29. Grant BD, Donaldson JG. Pathways and mechanisms of endocytotic recycling. *Mol Cell Biol*. 2009;10(9):597-604. doi:10.1038/nrm2755.Pathways.
30. Stanley AC, Lieu ZZ, Wall AA, et al. Recycling endosome-dependent and-independent mechanisms for IL-10 secretion in LPS-activated macrophages. *J Leukoc Biol*. 2012;92(6):1227-1239.
31. Lock JG, Stow JL. Rab11 in recycling endosomes regulates the sorting and basolateral transport of E-cadherin. *Mol Biol Cell*. 2005;16(4):1744-1755.
32. Palacios F, Price L, Schweitzer J, Collard JG, D'Souza-Schorey C. An essential role for ARF6-regulated membrane traffic in adherens junction turnover and epithelial cell migration. *EMBO J*. 2001;20(17):4973-4986.
33. Hulse RE, Swenson WG, Kunkler PE, White DM, Kraig RP. Monomeric IgG is neuroprotective via enhancing microglial recycling endocytosis and TNF-α. *J Neurosci*. 2008;28(47):12199-12211.
34. Stow JL, Manderson AP, Murray RZ. SNAREing immunity: the role of SNAREs in the immune system. *Nat Rev Immunol*. 2006;6(12):919-929.
35. Murray RZ, Kay JG, Sangermani DG, Stow JL. A role for the phagosome in cytokine secretion. *Science (80- )*. 2005;310(5753):1492-1495.
36. Li X, Maretzky T, Perez-Aguilar JM, et al. Structural modeling defines transmembrane residues in ADAM17 that are crucial for Rhbdf2/ADAM17-dependent proteolysis. *J Cell Sci*. 2017;(January):868-878. doi:10.1242/jcs.196436.
37. Horiuchi K, Kimura T, Miyamoto T, et al. Cutting edge: TNF-α-converting enzyme (TACE/ADAM17) inactivation in mouse myeloid cells prevents lethality from endotoxin shock. *J Immunol*. 2007;179(5):2686-2689.
38. Gooz M. ADAM-17: the enzyme that does it all. *Crit Rev Biochem Mol Biol*. 2010;45(2):146-169.
39. Friedmann E, Hauben E, Maylandt K, et al. SPPL2a and SPPL2b promote intramembrane proteolysis of TNFα in activated dendritic cells to trigger IL-12 production. *Nat Cell Biol*. 2006;8(8):843-848.
40. Adrain C, Zettl M, Christova Y, Taylor N, Freeman M. Tumor necrosis factor signaling requires iRhom2 to promote trafficking and activation of TACE. *Science (80- )*. 2012;335(6065):225-228.
41. Epelman S, Lavine KJ, Randolph GJ. Origin and Functions of Tissue Macrophages. *Immunity*. 2014;41(1):21-35. doi:10.1016/j.immuni.2014.06.013.
42. Schmid Hempel P, Schmid-Hempel P. *Evolutionary Parasitologythe Integrated Study of Infections, Immunology, Ecology, and Genetics*.; 2011.

43. Gordon S. The macrophage: past, present and future. *Eur J Immunol*. 2007;37(S1):S9-S17.
44. Epelman S, Lavine KJ, Beaudin AE, et al. Embryonic and adult-derived resident cardiac macrophages are maintained through distinct mechanisms at steady state and during inflammation. *Immunity*. 2014;40(1):91-104.
45. Zhang X, Mosser DM. Macrophage activation by endogenous danger signals. *J Pathol*. 2008;214(2):161-178.
46. Chen C-J, Kono H, Golenbock D, Reed G, Akira S, Rock KL. Identification of a key pathway required for the sterile inflammatory response triggered by dying cells. *Nat Med*. 2007;13(7):851-856.
47. Mackaness GB. Cellular immunity and the parasite. In: *Immunity to Blood Parasites of Animals and Man*. Springer; 1977:65-73.
48. Gordon S. Alternative activation of macrophages. *Nat Rev Immunol*. 2003;3(1):23-35.
49. Edwards JP, Zhang X, Frauwirth KA, Mosser DM. Biochemical and functional characterization of three activated macrophage populations. *J Leukoc Biol*. 2006;80(6):1298-1307.
50. James SL, Nacy C. Effector functions of activated macrophages against parasites. *Curr Opin Immunol*. 1993;5(4):518-523.
51. Chaussabel D, Semnani RT, McDowell MA, Sacks D, Sher A, Nutman TB. Unique gene expression profiles of human macrophages and dendritic cells to phylogenetically distinct parasites. *Blood*. 2003;102(2):672-681.
52. O'shea JJ, Murray PJ. Cytokine signaling modules in inflammatory responses. *Immunity*. 2008;28(4):477-487.
53. Martinez FO, Gordon S. The M1 and M2 paradigm of macrophage activation: time for reassessment. *F1000Prime Rep*. 2014;6:13. doi:10.12703/P6-13.
54. Mills CD, Kincaid K, Alt JM, Heilman MJ, Hill AM. M-1/M-2 macrophages and the Th1/Th2 paradigm. *J Immunol*. 2000;164(12):6166-6173.
55. Sinha P, Clements VK, Ostrand-Rosenberg S. Reduction of myeloid-derived suppressor cells and induction of M1 macrophages facilitate the rejection of established metastatic disease. *J Immunol*. 2005;174(2):636-645.
56. Mills C. M1 and M2 macrophages: oracles of health and disease. *Crit Rev Immunol*. 2012;32(6).
57. Stow JL, Low PC, Offenhäuser C, Sangermani D. Cytokine secretion in macrophages and other cells: pathways and mediators. *Immunobiology*. 2009;214(7):601-612.
58. Lucas M, Stuart LM, Savill J, Lacy-Hulbert A. Apoptotic cells and innate immune stimuli combine to regulate macrophage cytokine secretion. *J Immunol*. 2003;171(5):2610-2615.
59. Reefman E, Kay JG, Wood SM, et al. Cytokine secretion is distinct from secretion of cytotoxic granules in NK cells. *J Immunol*. 2010;184(9):4852-4862.
60. Pace JL, Russell SW, Torres BA, Johnson HM, Gray PW. Recombinant mouse gamma interferon induces the priming step in macrophage activation for tumor cell killing. *J Immunol*. 1983;130(5):2011-2013.
61. Schroder K, Hertzog PJ, Ravasi T, Hume DA. Interferon-γ: an overview of signals, mechanisms and functions. *J Leukoc Biol*. 2004;75(2):163-189.
62. Bouvier NM, Palese P. The biology of influenza viruses. *Vaccine*. 2008;26:D49-D53.
63. Hause BM, Collin EA, Liu R, et al. Characterization of a novel influenza virus in cattle and swine: proposal for a new genus in the Orthomyxoviridae family. *MBio*. 2014;5(2):e00031-14.
64. Tellier R. Review of Aerosol Transmission of Influenza A Virus-Volume 12, Number 11—November 2006-Emerging Infectious Disease journal-CDC. 2006.
65. Karron RA, Collins PL. Parainfluenza viruses. In: *Fields Virology: Sixth Edition*. Wolters Kluwer Health Adis (ESP); 2013.
66. Yoon S-W, Webby RJ, Webster RG. Evolution and ecology of influenza A viruses. In: *Influenza Pathogenesis and Control-Volume I*. Springer; 2014:359-375.
67. Tognotti E. Influenza pandemics: a historical retrospect. *J Infect Dev Ctries*. 2009;3(5):331-

334.
68. Brankston G, Gitterman L, Hirji Z, Lemieux C, Gardam M. Transmission of influenza A in human beings. *Lancet Infect Dis*. 2007;7(4):257-265.
69. te Velthuis AJW, Fodor E. Influenza virus RNA polymerase: insights into the mechanisms of viral RNA synthesis. *Nat Rev Microbiol*. 2016;14(8):479-493. doi:10.1038/nrmicro.2016.87.
70. Alexander DJ. An overview of the epidemiology of avian influenza. *Vaccine*. 2007;25(30):5637-5644.
71. Koel BF, Burke DF, Bestebroer TM, et al. Substitutions near the receptor binding site determine major antigenic change during influenza virus evolution. *Science (80- )*. 2013;342(6161):976-979.
72. Carrat F, Flahault A. Influenza vaccine: the challenge of antigenic drift. *Vaccine*. 2007;25(39):6852-6862.
73. Hensley SE, Das SR, Bailey AL, et al. Hemagglutinin receptor binding avidity drives influenza A virus antigenic drift. *Science (80- )*. 2009;326(5953):734-736.
74. Treanor J. Influenza vaccine—outmaneuvering antigenic shift and drift. *N Engl J Med*. 2004;350(3):218-220.
75. Dowdle WR. The origin of pandemic influenza viruses. *Science (80- )*. 1984;223:1402-1404.
76. Johnson NPAS, Mueller J. Updating the accounts: global mortality of the 1918-1920“ Spanish” influenza pandemic. *Bull Hist Med*. 2002;76(1):105-115.
77. Osterhaus A, Rimmelzwaan GF, Martina BEE, Bestebroer TM, Fouchier RAM. Influenza B virus in seals. *Science (80- )*. 2000;288(5468):1051-1053.
78. Bianchi E, Garsky V, Ingallinella P, et al. Influenza virus vaccine. March 2004.
79. Ritchey MB, Palese P, Kilbourne ED. RNAs of influenza A, B, and C viruses. *J Virol*. 1976;18(2):738-744.
80. Suarez D. Influenza A virus. *Anim Influ*. 2008:1-30.
81. Eisfeld AJ, Neumann G, Kawaoka Y. At the centre: influenza A virus ribonucleoproteins. *Nat Rev Microbiol*. 2015;13(1):28-41.
82. Noda T, Sagara H, Yen A, et al. Architecture of ribonucleoprotein complexes in influenza A virus particles. *Nature*. 2006;439(7075):490-492.
83. Noda T, Sugita Y, Aoyama K, et al. Three-dimensional analysis of ribonucleoprotein complexes in influenza A virus. *Nat Commun*. 2012;3:639.
84. Noda T, Kawaoka Y. Structure of influenza virus ribonucleoprotein complexes and their packaging into virions. *Rev Med Virol*. 2010;20(6):380-391.
85. Nayak DP, Hui EK-W, Barman S. Assembly and budding of influenza virus. *Virus Res*. 2004;106(2):147-165.
86. Rossman JS, Lamb RA. Influenza virus assembly and budding. *Virology*. 2011;411(2):229-236.
87. Jackson D, Lamb RA. The influenza A virus spliced messenger RNA M mRNA3 is not required for viral replication in tissue culture. *J Gen Virol*. 2008;89(12):3097-3101.
88. Muramoto Y, Noda T, Kawakami E, Akkina R, Kawaoka Y. Identification of novel influenza A virus proteins translated from PA mRNA. *J Virol*. 2013;87(5):2455-2462.
89. Samji T. Influenza A: Understanding the viral life cycle. *Yale J Biol Med*. 2009;82(4):153-159.
90. Watanabe T, Watanabe S, Kawaoka Y. Cellular networks involved in the influenza virus life cycle. *Cell Host Microbe*. 2010;7(6):427-439.
91. Huang Q, Sivaramakrishna RP, Ludwig K, Korte T, Böttcher C, Herrmann A. Early steps of the conformational change of influenza virus hemagglutinin to a fusion active state: stability and energetics of the hemagglutinin. *Biochim Biophys Acta (BBA)-Biomembranes*. 2003;1614(1):3-13.
92. Sun X, Whittaker GR. Role of the actin cytoskeleton during influenza virus internalization into polarized epithelial cells. *Cell Microbiol*. 2007;9(7):1672-1682.
93. König R, Stertz S, Zhou Y, et al. Human host factors required for influenza virus replication.

*Nature*. 2010;463(7282):813-817.
94. Chu VC, Whittaker GR. Influenza virus entry and infection require host cell N-linked glycoprotein. *Proc Natl Acad Sci*. 2004;101(52):18153-18158.
95. Skehel JJ, Wiley DC. Receptor binding and membrane fusion in virus entry: the influenza hemagglutinin. *Annu Rev Biochem*. 2000;69(1):531-569.
96. Desai TM, Marin M, Chin CR, Savidis G, Brass AL, Melikyan GB. IFITM3 restricts influenza A virus entry by blocking the formation of fusion pores following virus-endosome hemifusion. *PLoS Pathog*. 2014;10(4):e1004048.
97. Amorim MJ, Digard P. Influenza A virus and the cell nucleus. *Vaccine*. 2006;24(44):6651-6655.
98. Li X, Palese P. Characterization of the polyadenylation signal of influenza virus RNA. *J Virol*. 1994;68(2):1245-1249.
99. Sato SB, Kawasaki K, Ohnishi S-L. Hemolytic activity of influenza virus hemagglutinin glycoproteins activated in mildly acidic environments. *Proc Natl Acad Sci*. 1983;80(11):3153-3157.
100. Yoshimura A, Ohnishi S. Uncoating of influenza virus in endosomes. *J Virol*. 1984;51(2):497-504.
101. Kobiler O, Drayman N, Butin-Israeli V, Oppenheim A. Virus strategies for passing the nuclear envelope barrier. *Nucleus*. 2012;3(6):526-539.
102. Mühlbauer D, Dzieciolowski J, Hardt M, et al. Influenza virus-induced caspase-dependent enlargement of nuclear pores promotes nuclear export of viral ribonucleoprotein complexes. *J Virol*. 2015;89(11):6009-6021.
103. Robertson JS, Schubert M, Lazzarini RA. Polyadenylation sites for influenza virus mRNA. *J Virol*. 1981;38(1):157-163.
104. Hara K, Schmidt FI, Crow M, Brownlee GG. Amino acid residues in the N-terminal region of the PA subunit of influenza A virus RNA polymerase play a critical role in protein stability, endonuclease activity, cap binding, and virion RNA promoter binding. *J Virol*. 2006;80(16):7789-7798.
105. Reich S, Guilligay D, Pflug A, et al. Structural insight into cap-snatching and RNA synthesis by influenza polymerase. *Nature*. 2014;516(7531):361-366.
106. Dias A, Bouvier D, Crépin T, et al. The cap-snatching endonuclease of influenza virus polymerase resides in the PA subunit. *Nature*. 2009;458(7240):914-918.
107. Zheng H, Lee HA, Palese P, García-Sastre A. Influenza A virus RNA polymerase has the ability to stutter at the polyadenylation site of a viral RNA template during RNA replication. *J Virol*. 1999;73(6):5240-5243.
108. Whittaker GR, Helenius A. Nuclear import and export of viruses and virus genomes. *Virology*. 1998;246(1):1-23.
109. Hay AJ, Lomniczi B, Bellamy AR, Skehel JJ. Transcription of the influenza virus genome. *Virology*. 1977;83(2):337-355.
110. Hay AJ, Skehel JJ, McCauley J. Characterization of influenza virus RNA complete transcripts. *Virology*. 1982;116(2):517-522.
111. Moeller A, Kirchdoerfer RN, Potter CS, Carragher B, Wilson IA. Organization of the influenza virus replication machinery. *Science (80- )*. 2012;338(6114):1631-1634.
112. Lund E, Güttinger S, Calado A, Dahlberg JE, Kutay U. Nuclear export of microRNA precursors. *Science (80- )*. 2004;303(5654):95-98.
113. Fornerod M, Ohno M, Yoshida M, Mattaj IW. CRM1 is an export receptor for leucine-rich nuclear export signals. *Cell*. 1997;90(6):1051-1060.
114. Akarsu H, Burmeister WP, Petosa C, et al. Crystal structure of the M1 protein-binding domain of the influenza A virus nuclear export protein (NEP/NS2). *EMBO J*. 2003;22(18):4646-4655.
115. Ashton PR, Baxter I, Cantrill SJ, et al. Supramolecular daisy chains. *Angew Chemie Int Ed*. 1998;37(9):1294-1297.

116. Wang X, Hinson ER, Cresswell P. The interferon-inducible protein viperin inhibits influenza virus release by perturbing lipid rafts. *Cell Host Microbe*. 2007;2(2):96-105.
117. Martin K, Heleniust A. Nuclear transport of influenza virus ribonucleoproteins: the viral matrix protein (M1) promotes export and inhibits import. *Cell*. 1991;67(1):117-130.
118. Ali A, Avalos RT, Ponimaskin E, Nayak DP. Influenza virus assembly: effect of influenza virus glycoproteins on the membrane association of M1 protein. *J Virol*. 2000;74(18):8709-8719.
119. Vale-Costa S, Amorim MJ. Recycling endosomes and viral infection. *Viruses*. 2016;8(3):64.
120. Carrasco M, Amorim MJ, Digard P. Lipid Raft-Dependent Targeting of the Influenza A Virus Nucleoprotein to the Apical Plasma Membrane. *Traffic*. 2004;5(12):979-992.
121. Amorim MJ, Bruce EA, Read EKC, et al. A Rab11-and microtubule-dependent mechanism for cytoplasmic transport of influenza A virus viral RNA. *J Virol*. 2011;85(9):4143-4156.
122. Hall A. Small GTP-binding proteins and the regulation of the actin cytoskeleton. *Annu Rev Cell Biol*. 1994;10(1):31-54.
123. Momose F, Sekimoto T, Ohkura T, et al. Apical transport of influenza A virus ribonucleoprotein requires Rab11-positive recycling endosome. *PLoS One*. 2011;6(6):e21123.
124. Bruce EA, Digard P, Stuart AD. The Rab11 pathway is required for influenza A virus budding and filament formation. *J Virol*. 2010;84(12):5848-5859.
125. Vale-Costa S, Alenquer M, Sousa AL, et al. Influenza A virus ribonucleoproteins modulate host recycling by competing with Rab11 effectors. *J Cell Sci*. 2016;129(8):1697-1710.
126. McMahon HT, Gallop JL. Membrane curvature and mechanisms of dynamic cell membrane remodelling. *Nature*. 2005;438(7068):590-596.
127. Zimmerberg J, Kozlov MM. How proteins produce cellular membrane curvature. *Nat Rev Mol cell Biol*. 2006;7(1):9-19.
128. Barman S, Adhikary L, Chakrabarti AK, Bernas C, Kawaoka Y, Nayak DP. Role of transmembrane domain and cytoplasmic tail amino acid sequences of influenza a virus neuraminidase in raft association and virus budding. *J Virol*. 2004;78(10):5258-5269.
129. Marvin SA, Russier M, Huerta CT, Russell CJ, Schultz-Cherry S. Influenza overcomes cellular blocks to productively replicate impacting macrophage function. *J Virol*. 2016;91(2):JVI.01417-16. doi:10.1128/JVI.01417-16.
130. Steinhauer DA. Role of hemagglutinin cleavage for the pathogenicity of influenza virus. *Virology*. 1999;258(1):1-20.
131. Lazarowitz SG, Choppin PW. Enhancement of the infectivity of influenza A and B viruses by proteolytic cleavage of the hemagglutinin polypeptide. *Virology*. 1975;68(2):440-454.
132. Goraya MU, Wang S, Munir M, Chen JL. Induction of innate immunity and its perturbation by influenza viruses. *Protein Cell*. 2015;6(10):712-721. doi:10.1007/s13238-015-0191-z.
133. Guillot L, Le Goffic R, Bloch S, et al. Involvement of toll-like receptor 3 in the immune response of lung epithelial cells to double-stranded RNA and influenza A virus. *J Biol Chem*. 2005;280(7):5571-5580.
134. Pichlmair A, Schulz O, Tan CP, et al. RIG-I-mediated antiviral responses to single-stranded RNA bearing 5'-phosphates. *Science (80- )*. 2006;314(5801):997-1001.
135. Damjanovic D, Divangahi M, Kugathasan K, et al. Negative regulation of lung inflammation and immunopathology by TNF-α during acute influenza infection. *Am J Pathol*. 2011;179(6):2963-2976.
136. Belisle SE, Tisoncik JR, Korth MJ, et al. Genomic profiling of tumor necrosis factor alpha (TNF-α) receptor and interleukin-1 receptor knockout mice reveals a link between TNF-α signaling and increased severity of 1918 pandemic influenza virus infection. *J Virol*. 2010;84(24):12576-12588.
137. DeBerge MP, Ely KH, Enelow RI. Soluble, but not transmembrane, TNF-α is required during influenza infection to limit the magnitude of immune responses and the extent of immunopathology. *J Immunol*. 2014;192(12):5839-5851.
138. García-Sastre A, Egorov A, Matassov D, et al. Influenza A virus lacking the NS1 gene

replicates in interferon-deficient systems. *Virology*. 1998;252(2):324-330.
139. Gannagé M, Dormann D, Albrecht R, et al. Matrix protein 2 of influenza A virus blocks autophagosome fusion with lysosomes. *Cell Host Microbe*. 2009;6(4):367-380.
140. Wu S, Metcalf JP, Wu W. Innate immune response to influenza virus. *Curr Opin Infect Dis*. 2011;24(3):235-240.
141. Schlitzer A, Schultze JL. Tissue-resident macrophages [mdash] how to humanize our knowledge. *Immunol Cell Biol*. 2017;95(2):173-177. http://dx.doi.org/10.1038/icb.2016.82.
142. Nicol MQ, Dutia BM. The role of macrophages in influenza A virus infection. 2014;9:847-862.
143. Shapiro GI, Gurney T, Krug RM. Influenza virus gene expression: control mechanisms at early and late times of infection and nuclear-cytoplasmic transport of virus-specific RNAs. *J Virol*. 1987;61(3):764-773.
144. Pereira CF, Read EKC, Wise HM, Amorim MJ, Digard P. The influenza A virus NS1 protein promotes efficient nuclear export of unspliced viral M1 mRNA. *J Virol*. 2017;(May):JVI.00528-17. doi:10.1128/JVI.00528-17.
145. Boncompain G, Divoux S, Gareil N, et al. Synchronization of secretory protein traffic in populations of cells. *Nat Methods*. 2012;9(5):493-498.
146. Nair-Gupta P, Baccarini A, Tung N, et al. TLR signals induce phagosomal MHC-I delivery from the endosomal recycling compartment to allow cross-presentation. *Cell*. 2014;158(3):506-521.
147. Cox D, Lee DJ, Dale BM, Calafat J, Greenberg S. A Rab11-containing rapidly recycling compartment in macrophages that promotes phagocytosis. *Proc Natl Acad Sci*. 2000;97(2):680-685.
148. Aggarwal BB. Signalling pathways of the TNF superfamily: a double-edged sword. *Nat Rev Immunol*. 2003;3(9):745-756. doi:10.1038/nri1184.